


Article

Genome-Wide Identification, Characterization, and Expression Profiling of the Glutaredoxin Gene Family in Tea Plant (*Camellia sinensis*)

Dong Jiang ^{1,2}, Wenhai Yang ¹, Jianhui Pi ³, Guoqun Yang ¹, Yong Luo ⁴, Shenxiu Du ⁵, Ning Li ^{1,2} and Li-Jun Huang ^{1,*} 

¹ Key Laboratory of Cultivation and Protection for Non-Wood Forest Trees, College of Forestry, Central South University of Forestry and Technology, Changsha 410004, China

² Key Laboratory of Forest Bio-Resources and Integrated Pest Management for Higher Education in Hunan Province, Central South University of Forestry and Technology, Changsha 410004, China

³ Key Laboratory of Research and Utilization of Ethnomedicinal Plant Resources of Hunan Province, College of Biological and Food Engineering, Huaihua University, Huaihua 418008, China

⁴ School of Chemistry and Environmental Science, Xiangnan University, Chenzhou 423000, China

⁵ Biotechnology Research Institute, Chinese Academy of Agricultural Sciences, Beijing 100081, China

* Correspondence: nghua@126.com

Abstract: Glutaredoxins (GRXs) are a widely distributed group of small oxidoreductases that play an important role in responding to oxidative stress and maintaining redox homeostasis in living organisms. However, there has been no report on the GRX gene family in tea plants (*Camellia sinensis*). In this study, we conducted a systematic analysis of the CsGRX gene family in tea plants and identified a total of 86 CsGRX genes. Based on phylogenetic and conserved active site analyses, these genes were classified into four categories: CC-type, CPYC-type, CGFS-type, and GRL-type. These subtypes showed distinct characteristics in terms of gene structure, conserved motif, chromosome distribution, subcellular localization, *cis*-regulatory elements, and expression pattern, indicating functional differences among CsGRX family members. Collinearity analysis showed that the CsGRX family may have undergone member expansion using tandem and segmental duplication along with overwhelmingly strict purifying selection. Protein tertiary structure analysis supported the conserved site-specific binding of CsGRX family members to glutathione. Protein interaction network analysis revealed that CsGRX may interact with glutathione reductase (GR), 2-Cys Peroxiredoxin BAS1, TGA3, and others to participate in the oxidative stress response in tea plants. GO and KEGG enrichment analyses also supported the important role of the CsGRX family in maintaining intracellular redox homeostasis. Expression analysis based on RNA-seq revealed differential expression patterns of CsGRX genes under drought, cold stress, and in different tissues, which were further confirmed by RT-qPCR analysis, indicating their broad-spectrum functionality. This study provides a new perspective for further exploring the evolution and molecular functions of specific CsGRX genes.

Keywords: CsGRX; glutaredoxin; *Camellia sinensis*; oxidoreductase enzymes; oxidative stress; selection pressure; collinearity; gene expression



Citation: Jiang, D.; Yang, W.; Pi, J.; Yang, G.; Luo, Y.; Du, S.; Li, N.; Huang, L.-J. Genome-Wide Identification, Characterization, and Expression Profiling of the Glutaredoxin Gene Family in Tea Plant (*Camellia sinensis*). *Forests* **2023**, *14*, 1647. <https://doi.org/10.3390/f14081647>

Academic Editor: Donald L. Rockwood

Received: 23 July 2023

Revised: 8 August 2023

Accepted: 10 August 2023

Published: 15 August 2023



Copyright: © 2023 by the authors. Licensee MDPI, Basel, Switzerland. This article is an open access article distributed under the terms and conditions of the Creative Commons Attribution (CC BY) license (<https://creativecommons.org/licenses/by/4.0/>).

1. Introduction

In response to environmental stresses, plants must face various adversity stimuli and evolve multiple adaptive and coping mechanisms. When cells are exposed to external stimuli and internal metabolic burdens, they produce or accumulate large amounts of reactive oxygen species (ROS), including hydrogen peroxide (H₂O₂), singlet oxygen (¹O₂), hydroxyl radical (HO[•]) and superoxide radical (O₂^{•−}), among others [1–3]. The accumulation of these ROS can cause oxidative damage to macromolecules such as cell membranes, proteins, and DNA, thus threatening the normal physiological metabolism and growth and development of the cell [2,4,5]. To cope with the challenge of oxidative stress,

plants have evolved a sophisticated ROS scavenging system, which includes various redox enzymes and enzymatic systems [6,7]. The main ROS scavenging enzymes include superoxide dismutase (SOD), peroxidase (POD), catalase (CAT), ascorbate peroxidase (APX), glutathione reductase (GR), glutathione peroxidase (GPX), and glutathione S-transferase (GST) [8,9]. These enzymes can convert ROS into harmless substances, thus protecting cells from oxidative damage. For example, SOD can convert the produced $O_2^{\cdot-}$ into H_2O_2 , which can be further converted into water via the coordinated action of CAT, APX, and other enzymes. Meanwhile, MSRA and GR can participate in ROS scavenging as reducing agents, with GR primarily participating in the ROS scavenging process via the glutathione cycle system [9,10]. In addition to these ROS-scavenging enzymes, some protein families in plants play important roles, such as the glutaredoxin (GRX) family and thioredoxin (TRX) family [11,12], which can scavenge ROS in the form of reducing agents and participate in signal transduction cascade to regulate gene regulation [10]. Therefore, the ROS scavenging system in plants is a complex network, including multiple redox enzymes and protein families, which maintain the redox balance and normal growth and development of the plant through intertwined and coordinated regulation [13].

GRXs are a class of small molecular weight proteins with reductase activities that are widely distributed in eukaryotes, bacteria, and archaea [14]. As part of the cell's intracellular redox buffering system, GRX plays an important role in the oxidative-reductive reaction by reducing thiols together with the reducing agent NADPH and the reducing system [15]. Glutathione reductase (GR), by reducing NADPH to $NADP^+$ with the help of reduced glutathione, helps maintain the cellular redox homeostasis level of GRX [16]. GRX combats oxidative stress through various mechanisms, such as reducing PRXs to control the level of peroxides or directly reducing peroxides or dehydroascorbate [17]. In addition, GRX can manipulate glutathionylation or deglutathionylation mechanisms to protect the thiol groups of other enzymes [15,16]. Through these pathways, GRX can help cells maintain redox homeostasis and reduce the impact of oxidative stress on cells [14]. GRX is typically composed of a conserved active site motif cys-x-x-ser (monothiol GRX) or cys-x-x-cys (dithiol GRX) that directly participates in the reduction reaction [16,18]. GRX is involved in many cellular processes, such as DNA synthesis, protein folding, iron-sulfur cluster formation, and cell signal transduction, and plays an important protective role in living organisms by resisting oxidative stress and maintaining the stability of cell structure and function [19–22]. There are multiple subtypes of GRX in plants, which can be classified into four categories based on phylogenetic relationships and conserved active site motifs: CC-type, CPYC-type, CGFS-type, and GRL (GRX-like)-type [23]. The GRX gene family has been systematically identified and analyzed in various plants, such as *Arabidopsis* [17], rice [23], poplar [24], cotton [25], common bean [26], and banana [27]. Among them, CGFS-type and CPYC-type have been reported in both prokaryotes and eukaryotes, while CC-type has only been identified in the plant kingdom [28–30].

Camellia sinensis, a perennial evergreen tree belonging to the Theaceae family, is used to produce tea from both its fresh and dried leaves [31]. The type and flavor of tea varies depending on the region, season, climate, and method of production [32]. Tea contains various nutrients and bioactive compounds, such as caffeine, catechins, flavonoids, and amino acids, which have health benefits such as antioxidant, antibacterial, antiviral, and lipid-lowering effects [33–35]. Consequently, tea has become one of the most popular beverages worldwide. However, tea plants are often exposed to various abiotic stresses during their growth and development, such as drought, cold, salt, alkaline, and heavy metals, which pose a serious threat to tea yield and quality [36]. Therefore, identifying and analyzing genes that respond to different abiotic stresses in tea plants is necessary. The GRX gene family has been identified with important roles in various plants, but its biological function in tea plants is unclear. In this study, to investigate the defense response and regulatory mechanisms of GRX genes in tea plants, we systematically identified 86 *CsGRX* genes by analyzing the tea plant genome and conducted chromosomal distribution, subcellular localization, phylogenetic analysis, and protein–protein interaction (PPI)

network analysis. In addition, we also determined the differential expression of CsGRX genes in different tissues and under multiple abiotic stresses. Our results provide clues for further analysis and validation of the biological and molecular functions of CsGRX genes and their antioxidant effects under various oxidative stresses.

2. Materials and Methods

2.1. Plant Materials and Growth Conditions

The tea plants (*Camellia sinensis* var. *sinensis* cv. Shuchazao) were grown at the nursery base of Central South University of Forestry and Technology, Changsha City, China. Different tissues of tea plants were collected and rapidly frozen in liquid nitrogen for tissue-specific analysis of CsGRX gene expression. Two-year-old tea plants with consistent growth vigor were selected for treatment with NaCl (100 mM), 20% polyethylene glycol (PEG 6000), or 0.2 mM salicylic acid (SA). The seedlings were then placed in a growth chamber at 23 °C with a 16 h photoperiod of 10,000 lux light intensity followed by 8 h of darkness. Leaf and root tissues were collected at different time points, rapidly frozen in liquid nitrogen, and stored at −80 °C until further use. Each experiment was performed with three biological replicates.

2.2. Identification of Glutaredoxin Genes in the *Camellia sinensis* Genome

The genome sequence data for the tea plant were obtained from the Tea Plant Genome Database [37]. The genome sequence data for *Arabidopsis thaliana* were obtained from the TAIR database (<https://www.arabidopsis.org/>) (accessed on 2 March 2023). The genome sequence data for *Glycine max*, *Vitis vinifera*, *Solanum tuberosum*, and *Sorghum bicolor* were obtained from the NCBI database (<https://www.ncbi.nlm.nih.gov/>) (accessed on 2 March 2023). The genome sequence data for *Populus trichocarpa* were obtained from the Phytozome database (<https://phytozome-next.jgi.doe.gov/>) (accessed on 2 March 2023). The genome sequence data for *Oryza sativa* were obtained from the Rice Genome Database (<http://rice.uga.edu/>) (accessed on 2 March 2023). Firstly, using the GRX protein sequences from *Arabidopsis thaliana* and tea plant as templates, BLASTP search was performed against the tea plant whole-genome sequence to collect all sequences with an E-value below 1×10^{-5} . Subsequently, the Hidden Markov Model (HMM) profile of the GRX conserved domain (PF00462) was downloaded from the PFAM database (<http://pfam-legacy.xfam.org/>) (accessed on 11 March 2023) and used to search against the tea plant proteome data using HMMER software (v3.0) to obtain putative tea plant GRX genes. The putative tea plant GRX genes obtained from both the BLASTP search and HMMER search were combined, redundant sequences were removed, and the conserved domain of all putative tea plant GRX proteins were examined using the NCBI-CDD tool (<https://www.ncbi.nlm.nih.gov/cdd/>) (accessed on 12 March 2023), PFAM database (<http://pfam-legacy.xfam.org/>) (accessed on 15 March 2023), and SMART (Simple Modular Architecture Research Tool, <http://smart.embl.de/>) (accessed on 16 March 2023) to identify all genes containing the Glutaredoxin (PF00462) domain.

2.3. The Chromosomal Localization of CsGRX Genes

The final set of 86 CsGRX protein-coding sequences was extracted from the tea plant genome file downloaded from the tea plant database for chromosome localization analysis. Graphical representation was performed using TBtools software (v1.120) [38].

2.4. Physicochemical Characteristics and Subcellular Localization of CsGRX Proteins

The 86 CsGRX protein sequences were analyzed using the ProtParam tool available on the ExPASy database [39]. Subcellular localization prediction of the 86 CsGRX proteins was performed using the WOLF PSORT [40].

2.5. The Phylogenetic Analysis and Sequence Alignment

The GRX protein sequences of *Arabidopsis thaliana* were downloaded from the TAIR database, and the identified 86 CsGRX protein sequences were aligned using MUSCLE in MEGA X software [41]. A phylogenetic tree was constructed using the Neighbor-Joining (NJ) method, Poisson model, Uniform Rates, Pair-wise deletion, and 1000 bootstrap replicates. The resulting tree was visualized using Itol [42]. The sequence alignment was performed using the Clustal Omega tool (<https://www.ebi.ac.uk/Tools/msa/clustalo/>) (accessed on 16 March 2023), and the alignment result was imported into Jalview software (v2.11.2.7) for further refinement [43,44].

2.6. Structural and Protein–Protein Interaction Network of CsGRX Proteins

The MEME online program was used for motif analysis of CsGRX proteins, and the location of the glutaredoxin-conserved domain was obtained from the InterPro database. The structural information of 86 CsGRX genes was extracted from the genome data and visualized using TBtools software (v1.120) for phylogenetic analysis, motif analysis, glutaredoxin-conserved domain location, and gene structure [38]. To determine the tertiary structure of the 86 identified CsGRX proteins, one suitable member was selected from each of the three classical CsGRX subtypes, and their protein sequences were submitted to the SWISS-MODEL tool in ExPASy to search for a Glutaredoxin model [45]. The 3D structure was then visualized using the model with the highest match. The protein–protein interaction (PPI) network of CsGRXs was analyzed with the STRING database. The analysis results were then imported into Cytoscape (v3.9.1) software for visualization [46].

2.7. Gene Duplication and Collinearity, and Selective Pressure Calculation

The MCScanX was used to analyze the duplication patterns and collinearity relationships of GRX genes within and between tea tree species [47]. The results were visualized using TBtools (v1.120), and the Ka/Ks ratio of synonymous and non-synonymous substitutions was calculated for orthologous gene pairs to study selection pressure [38].

2.8. Analysis of cis-Acting Elements in the Promoter Region

The promoter region refers to the 2000 bp sequence upstream of the translation initiation codon (ATG), which was obtained from the tea genome data file and submitted to the PlantCARE online program (<https://bioinformatics.psb.ugent.be/webtools/plantcare/html/>) (accessed on 22 March 2023) to identify cis-acting regulatory elements [48].

2.9. GO and KEGG Enrichment Analysis

The functional classification and KEGG pathway enrichment analysis of 86 CsGRX genes were performed using the EGGNOG-MAPPER tool [49]. Gene functions were categorized into biological processes, cellular components, and molecular functions.

2.10. RNA-seq-Based Expression Analysis of CsGRX Genes and Real-Time Quantitative PCR

The gene expression data of *Camellia sinensis* var. *sinensis* cv. Shuchazao were obtained from the Tea Plant Information Archive (TPIA) database and visualized the results using TBtools (v1.120) [38]. The expression levels of selected CsGRX genes in different tissues and in response to various abiotic stresses were determined using reverse transcription-quantitative polymerase chain reaction (RT-qPCR). The Plant RNA Extraction Kit (Tiangen, Beijing, China) was used to isolate total RNA from different parts of tea plants to verify tissue-specific expression, while tea roots and leaves obtained under different stresses were used to analyze gene expression under different stresses. Complementary DNA (cDNA) was synthesized by reverse transcription using M-MuLV reverse transcriptase (Sangon, Shanghai, China). The relative quantification method ($2^{-\Delta\Delta CT}$) was employed to evaluate the quantitative variation. Each independent sample was analyzed at least three times. The *GAPDH* gene was used as a reference gene. CsGRX gene-specific primers were designed using Primer Premier 6.0 software. The primer sequences are listed in Table S9.

3. Results

3.1. Identification, Classification, and Physicochemical Properties of the CsGRX Gene Family

To identify GRX genes in tea plants, we first used GRX genes from Arabidopsis and rice as screening query materials and conducted BLASTP searches in the tea plant genome. The results were then compiled, and redundancies were removed. Next, we downloaded the HMM model PF00462 of glutaredoxin from the InterPro database as the query condition and searched the tea plant genome using HMMER 3.0. The retrieval results were combined with the BLASTP results, redundancies were removed, and the sequences were submitted to InterPro, SMART, and NCBI-CDD databases to search for the presence of conserved domains in order to verify the reliability of these CsGRX genes.

Previous studies have shown that glutaredoxins in plants can be classified into four subtypes based on their conserved active sites, including CC-type, CPYC-type, CGFS-type, and GRL-type. Through sequence alignment and conserved active site analysis of the 86 CsGRX protein sequences, we found that these proteins can also be classified into these four subtypes (Figures 1 and 2, Table 1). Specifically, CC-type members are the most abundant (37), followed by GRL-type (27), CGFS-type (14), and CPYC-type (8). Using full-length protein sequences for sequence alignment, CC-type, CPYC-type, and CGFS-type, the three classic subtypes all contain conserved active sites, as shown in Figure 1. Specifically, the conserved active site of 37 CC-type members is CCMC, except for CsGRX24, CsGRX33, CsGRX50, and CsGRX56, which have less conserved active sites. For CPYC-type, the conserved active site varies more. Among them, CsGRX7, CsGRX8, and CsGRX55 have strictly conserved CPYC motifs, while other members have C[P/S/G][Y/F][C/S] motifs. In contrast, the CGFS-type has the highest conservation of active sites. Except for one amino acid residue change in CsGRX27 and CsGRX28, all other members have strictly conserved CGFS motifs. GRL-type does not have typical conserved active sites. Subsequently, we divided the identified 86 CsGRX sequences into two categories based on their subtypes, i.e., GRX types with conserved active sites and GRL types without conserved active sites, and named them according to their position order on the chromosome. The GRX genes located on the unmapped scaffold were also arranged in order.

We conducted a physicochemical property analysis of 86 CsGRX proteins using the ProtParam tool in ExPASy (Table 1). The protein sequence length of CsGRXs ranged from 101 to 790 amino acids, with a molecular weight ranging from 10.8 kDa to 88.89 kDa (Table 1). The estimated theoretical isoelectric point (pI) values ranged from 4.56 to 9.90. Moreover, the Aliphatic Index scores varied greatly, with 20 members having an Aliphatic Index greater than 100 and 7 members having an Aliphatic Index less than 70. All GRL-type and CGFS-type members had an Aliphatic Index of less than 100. We also predicted the Instability Index of these proteins, with 66 members predicted to be stable and the remaining 20 members predicted to be unstable. Among the 27 GRL-type members, all except CsGRL4 and CsGRL23 were predicted to be stable. For the Grand average of hydropathicity (GRAVY), all GRL-type members and most of the CGFS-type members had negative scores, while most CC-type members had positive scores. Finally, we predicted the Signal Peptide of all CsGRXs and found that only CsGRX1, CsGRX7, CsGRX8, and CsGRX55, belonging to the CPYC-type, had a Signal Peptide, while the others did not.

Using the WoLF PSORT program (Advanced Protein Subcellular Localization Prediction Tool), we predicted the subcellular localization of all 86 CsGRXs (Table 1, Figure S1). The results showed that all CsGRX proteins were present in cellular compartments, which is consistent with the function of GRXs and with previous studies in Arabidopsis and rice [23]. CsGRXs were located in chloroplasts, cytoplasm, nucleus, mitochondria, or extracellular regions. Previous studies have shown that many plant GRXs function in plastids and chloroplasts [50], and in our study, the largest number of CsGRXs (33) were located in chloroplasts, while 16 CsGRXs were in the cytoplasm, indirectly confirming previous research results. Interestingly, we found that all CsGRXs were not necessarily localized to specific locations within the cell but were distributed across multiple organelles. For example, we predicted two CsGRXs in the chloroplast/extracellular location, two members in the

chloroplast/cytoplasm location, and two members in the chloroplast/nucleus/extracellular location. These results suggest that CsGRXs may be involved in biological processes that span multiple organelles [51,52].

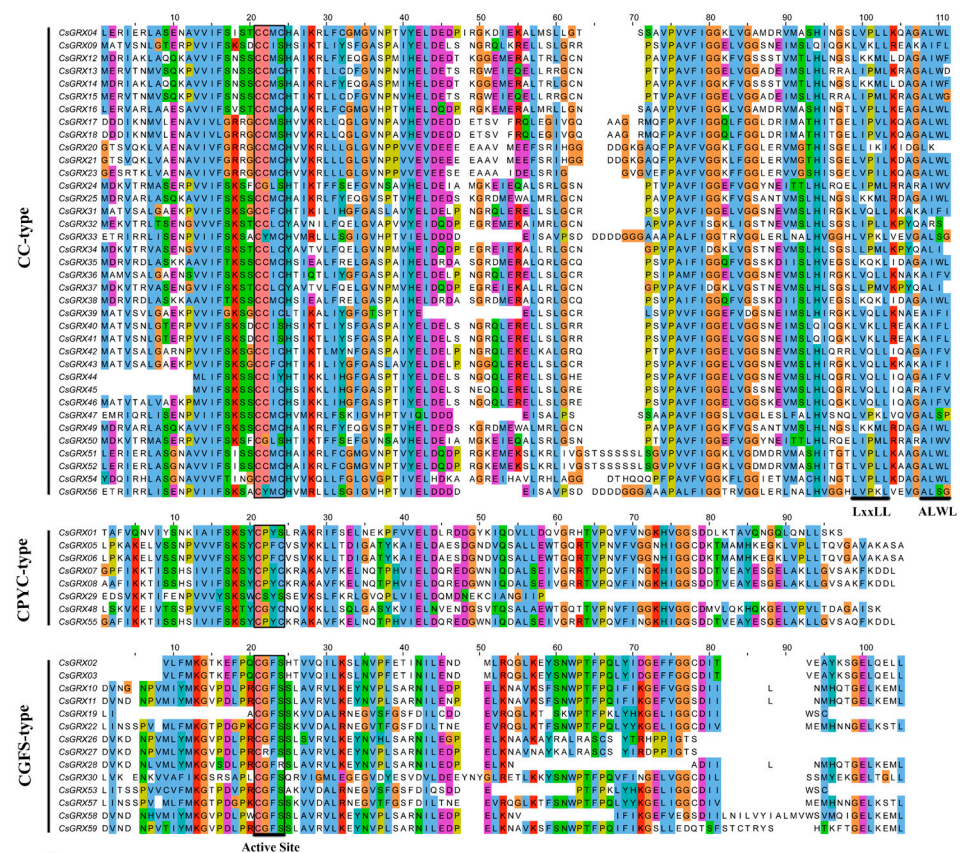


Figure 1. Multiple alignments of amino acid sequences of GRX proteins in *Camellia sinensis* by Clustal Omega and Jalview tools. Sites marked with the same color indicate that amino acid residues are the same or have high homology. The conservative active sites of the three subtypes of CC-type, CPYC-type, and CGFS-type are framed in black rectangles and marked in the lower part of the sequence, and the LxxLL and ALWL sites unique to CC-type are also labeled in the lower part of the sequence.

3.2. Multiple Sequence Alignment and Phylogenetic Analysis of CsGRXs

We examined the conservation of active sites, structural domains, and motifs of three classical GRX subtypes using multiple sequence alignment. Specifically, we used the Clustal Omega program to align the protein sequences of 86 CsGRX proteins and visualized the alignment results using Jalview (Figure 1). In all three classical subtypes, we found that all members had a conserved active site of four amino acid residues, starting with cysteine. Among the 37 CC-type members, 15 members had the CCMC active site, five members had the CCIC active site, four members had the CCMS active site, and other members had different active sites such as CCIS, CCLC, CCLS, CCFC, CCIY, and CYMC. In the CPYC-type subtype, three of the eight members had the conserved CPYC active site, while the rest had different active sites such as CPYS, CPFC, CSYS, and CGYC. For the CGFS-type subtype, all members, except CsGRX27 (CRFS) and CsGRX28 (CGFR), had a strictly conserved CGFS active site. Furthermore, we also found conserved motifs, such as LxxLL and the C-terminal ALWL motif, in the CC-type subtype. The former plays a role in inhibiting the function of genes in flower development and in mediating the promoter activity of *ORA59* (OCTADECANOID-RESPONSIVE ARABIDOPSIS AP2/ERF-domain protein 59), while the latter is a key site determining the interaction between CC-type glutaredoxins and TGA transcription factors, playing an important role in regulating plant growth and

development [53,54]. In addition, we explored the evolutionary relationship of the CsGRX gene family. Specifically, we used the full-length protein sequences of 86 CsGRXs and 48 AtGRXs to construct a phylogenetic tree based on multiple sequence alignment using the Neighbor–Joining (NJ) method in MEGA X (Figure 2). The results showed that GRX proteins could be divided into four branches, with members of the same subtype located adjacent to each other on the evolutionary tree, consistent with the previous classification results of CsGRX subtypes [23].

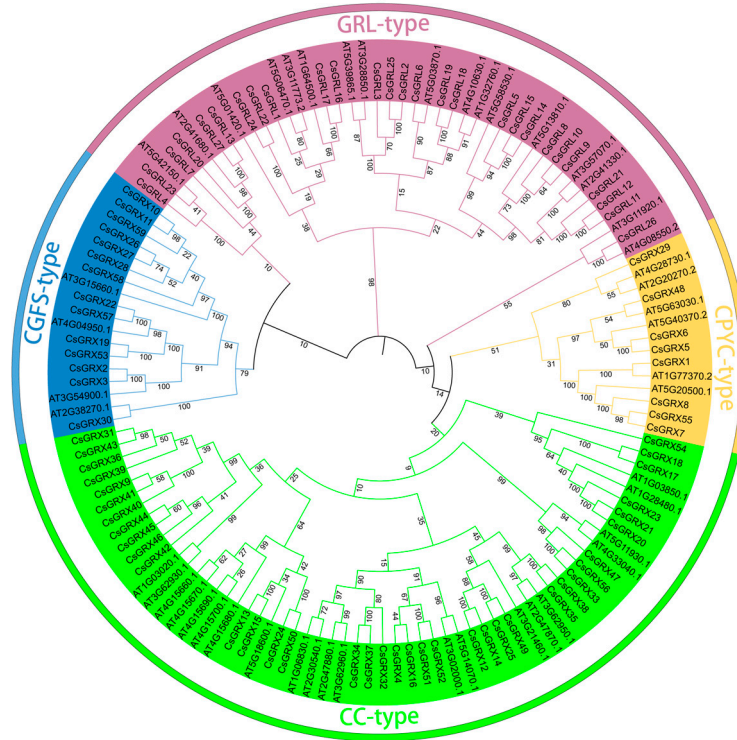


Figure 2. Phylogenetic analysis of GRX homologous proteins from *C. sinensis* and *A. thaliana*. The MEGAX with the Neighbor–Joining method was used to conduct the phylogenetic tree. The four subtypes are color-coded separately.

Table 1. Molecular feature of GRX genes identified in *Camellia sinensis*.

Gene ID	Rename	Class	Redox Site	Number of Amino Acid	Molecular Weight	Theoretical pI	Instability Index	Aliphatic Index	Grand Average of Hydrophobicity	Signal Peptide	Subcellular Localization
CSS0048558.1	CsGRL1	GRL		306	35,048.47	4.78	59.6	72.91	−0.647	NO	cyto
CSS0027383.1	CsGRX1	CPYC	CPYS	136	15,168.58	9.59	24.34	110.96	0.022	YES	chlo
CSS0049990.1	CsGRL2	GRL		554	61,464.34	6.45	44.24	68.12	−0.59	NO	mito
CSS0009163.1	CsGRX2	CGFS	CGFS	183	20,212.42	8.59	52.8	92.73	0.093	NO	chlo
CSS0032266.1	CsGRX3	CGFS	CGFS	180	19,939.17	8.8	52.3	93.72	0.091	NO	chlo
CSS0025130.1	CsGRX4	CC	CCMC	171	18,675.87	6.99	51.41	103.16	0.379	NO	chlo
CSS0002931.1	CsGRX5	CPYC	CPFC	107	11,293.11	7.71	36.42	92.9	0.116	NO	chlo
CSS0012888.1	CsGRX6	CPYC	CPFC	107	11,293.11	7.71	36.42	92.9	0.116	NO	chlo
CSS0026367.1	CsGRL3	GRL		379	42,509.94	5.02	46.98	71.93	−0.539	NO	cyto
CSS0010326.1	CsGRX7	CPYC	CPYC	130	14,375.56	6.28	44.52	94.46	−0.075	YES	extr
CSS0046074.1	CsGRX8	CPYC	CPYC	136	15,012.13	5.37	50.08	91.76	−0.125	YES	extr
CSS0016648.1	CsGRL4	GRL		341	38,093.2	8.25	37.71	76.66	−0.38	NO	chlo
CSS0038944.1	CsGRL5	GRL		252	28,391.42	8.91	63.97	69.6	−0.385	NO	nucl/mito
CSS0032078.1	CsGRL6	GRL		396	44,052.63	8.66	56.06	80.63	−0.445	NO	nucl
CSS0023185.1	CsGRL7	GRL		332	36,872.65	8.78	43.29	78.67	−0.221	NO	chlo
CSS0037319.1	CsGRX9	CC	CCIS	102	11,078.99	9.1	45.03	113.73	0.23	NO	nucl
CSS0022165.1	CsGRX10	CGFS	CGFS	186	20,565.26	6.19	48.57	76.02	−0.402	NO	mito
CSS0043406.1	CsGRX11	CGFS	CGFS	186	20,630.4	6.97	50.49	78.66	−0.378	NO	mito
CSS0041487.1	CsGRX12	CC	CCMS	102	11,074.96	8.54	41.99	88.04	0.128	NO	chlo
CSS0000241.1	CsGRX13	CC	CCMC	268	29,732.94	5.77	56.28	91.27	−0.189	NO	chlo

Table 1. Cont.

Gene ID	Rename	Class	Redox Site	Number of Amino Acid	Molecular Weight	Theoretical pI	Instability Index	Aliphatic Index	Grand Average of Hydrophobicity	Signal Peptide	Subcellular Localization
CSS0023854.1	CsGRX14	CC	CCMS	102	11,074.96	8.54	41.99	88.04	0.128	NO	chlo
CSS0017711.1	CsGRX15	CC	CCMC	288	31,658.95	5.2	49.55	87.99	−0.187	NO	chlo
CSS0045505.1	CsGRX16	CC	CCMC	129	14,097.69	8.71	37.62	94.42	0.25	NO	chlo
CSS0033754.1	CsGRL8	GRL		273	30,536.03	9.08	46.22	78.46	−0.397	NO	chlo/nucl/extr
CSS0008671.1	CsGRL9	GRL		273	30,536.03	9.08	46.22	78.46	−0.397	NO	chlo/nucl/extr
CSS0018532.1	CsGRX17	CC	CCMS	145	15,647.99	5.74	46.84	96.76	−0.02	NO	nucl
CSS0005014.1	CsGRX18	CC	CCMS	174	18,944.78	7.06	49.72	89.6	−0.145	NO	chlo
CSS0022827.1	CsGRX19	CGFS	CGFS	372	41,224.35	5.37	38.39	84.89	−0.148	NO	nucl
CSS0021697.1	CsGRX20	CC	CCMC	144	15,207.66	6.41	40.44	96.81	0.174	NO	chlo
CSS0048516.1	CsGRX21	CC	CCMC	146	15,334.72	5.76	46.88	94.86	0.209	NO	chlo
CSS0049641.1	CsGRX22	CGFS	CGFS	492	54,012.62	5.16	37.98	83.94	−0.274	NO	nucl
CSS0047198.1	CsGRX23	CC	CCMC	122	12,921.96	6.1	52.86	102.13	0.311	NO	chlo
CSS0036569.1	CsGRX24	CC	CGLS	102	11,382.21	6.83	43.55	93.63	0.112	NO	cyto
CSS0013953.1	CsGRX25	CC	CCMC	102	11,199.17	9.07	44.36	88.92	0.116	NO	chlo
CSS0016276.1	CsGRX26	CGFS	CGFS	165	18,451.98	9.9	55.02	70.97	−0.505	NO	mito
CSS0038997.1	CsGRX27	CGFS	CRFS	144	16,348.72	9.4	42.93	74.51	−0.406	NO	mito
CSS0032119.1	CsGRX28	CGFS	CGFR	131	14,826.94	8.76	46.95	78.17	−0.647	NO	mito
CSS0024990.1	CsGRX29	CPYC	CSYS	127	14,195.37	9.39	40.18	82.05	−0.091	NO	chlo
CSS0017181.1	CsGRL10	GRL		211	23,772.41	9.59	41.16	92.27	−0.165	NO	cyto
CSS0009561.1	CsGRX30	CGFS	CGFS	301	33,085.73	6.97	42.44	87.34	−0.325	NO	chlo
CSS0024807.1	CsGRL11	GRL		388	43,518.14	8.06	52.43	65.75	−0.576	NO	chlo
CSS0019682.1	CsGRL12	GRL		388	43,464.05	8.23	52.73	65.49	−0.584	NO	chlo
CSS0040554.1	CsGRL13	GRL		531	58,292.39	6.35	44.42	87.76	−0.233	NO	chlo
CSS0014693.1	CsGRX31	CC	CCFC	102	10,893.98	8.8	27.98	117.55	0.514	NO	cyto
CSS0014227.1	CsGRL14	GRL		251	27,892.93	8.8	63.61	77.25	−0.296	NO	nucl
CSS0026515.1	CsGRL15	GRL		251	27,892.93	8.8	63.61	77.25	−0.296	NO	nucl
CSS0019712.1	CsGRX32	CC	CCLC	101	11,003.9	5.75	39.45	103.17	0.25	NO	chlo
CSS0002577.1	CsGRX33	CC	CYMC	133	13,931.94	4.56	43.27	115.04	0.28	NO	cyto
CSS0015651.1	CsGRL16	GRL		382	42,528.53	7	43.97	69.08	−0.688	NO	cyto
CSS0012730.1	CsGRL17	GRL		382	42,514.46	6.64	44.09	69.08	−0.687	NO	cyto
CSS0047503.1	CsGRL18	GRL		331	36,277.66	6.03	51.19	77.28	−0.254	NO	cyto
CSS0041979.1	CsGRL19	GRL		330	36,186.6	6.12	52.39	77.82	−0.243	NO	cyto/cyto_nucl
CSS0027906.1	CsGRL20	GRL		143	16,386.96	6.11	40.28	81.82	−0.48	NO	cyto
CSS0026288.1	CsGRL21	GRL		408	45,057.75	5.51	55.5	72.82	−0.448	NO	chlo
CSS0026741.1	CsGRL22	GRL		314	35,015.07	6.31	44.95	83.76	−0.296	NO	mito
CSS0014972.1	CsGRX34	CC	CCLC	101	10,946.85	5.21	29.93	108.91	0.308	NO	chlo/cyto
CSS0043242.1	CsGRX35	CC	CCMC	102	11,070.86	7.71	43.35	97.65	0.072	NO	chlo
CSS0005766.1	CsGRX36	CC	CCIC	102	10,925.88	6.7	35.43	111.86	0.467	NO	chlo
CSS0036816.1	CsGRX37	CC	CCLC	101	10,932.82	5.21	30.49	107.92	0.312	NO	chlo/cyto
CSS0040033.1	CsGRX38	CC	CCMC	102	11,070.86	7.71	43.35	97.65	0.072	NO	chlo
CSS0043621.1	CsGRX39	CC	CCIC	104	11,368.43	5.7	26.93	108.65	0.696	NO	cyto/extr
CSS0038141.1	CsGRX40	CC	CCIS	102	11,079.93	7.79	42.67	113.73	0.234	NO	nucl
CSS0039696.1	CsGRX41	CC	CCIS	102	11,079.93	7.79	42.67	113.73	0.234	NO	nucl
CSS0042247.1	CsGRX42	CC	CCIC	102	10,968.92	8.57	42.35	110.88	0.359	NO	cyto
CSS0048300.1	CsGRX43	CC	CCFC	102	10,820.88	8.41	26.28	117.55	0.573	NO	cyto
CSS0016363.1	CsGRX44	CC	CCY	133	14,662.92	5.45	40.77	100.38	0.106	NO	extr
CSS0003005.1	CsGRX45	CC	CCIC	114	12,654.82	6.81	43.63	107.72	0.236	NO	extr
CSS0037431.1	CsGRX46	CC	CCIC	104	11,108.1	6.26	31.02	117.12	0.465	NO	cyto
CSS0027361.1	CsGRX47	CC	CCMC	134	14,214.48	6.17	52.24	110.52	0.314	NO	chlo
CSS0047807.1	CsGRX48	CPYC	CGYC	120	12,710.54	8.42	29.75	84.33	−0.119	NO	chlo
CSS0013276.1	CsGRL23	GRL		334	37,421.71	8.75	39.15	89.37	−0.24	NO	chlo
CSS0000523.1	CsGRX49	CC	CCMC	102	11,199.17	9.07	44.36	88.92	0.116	NO	chlo
CSS0035289.1	CsGRX50	CC	CGLS	102	11,382.21	6.83	43.55	93.63	0.112	NO	cyto
CSS0044719.1	CsGRX51	CC	CCMC	141	14,816.24	8.78	46.5	98.09	0.314	NO	chlo/extr
CSS0005657.1	CsGRX52	CC	CCMC	141	14,816.24	8.78	46.5	98.09	0.314	NO	chlo/extr
CSS0022772.1	CsGRL24	GRL		318	35,478.76	6.42	43.85	88.84	−0.255	NO	mito
CSS0013622.1	CsGRX53	CGFS	CGFS	403	44,436.07	5.05	40.05	86.33	−0.072	NO	nucl
CSS0006151.1	CsGRL25	GRL		557	61,591.53	6.68	44.28	67.76	−0.584	NO	mito
CSS0040793.1	CsGRX54	CC	CCMC	138	14,501.79	6.64	53.86	95.36	0.213	NO	cyto
CSS0034533.1	CsGRX55	CPYC	CPYC	130	14,349.48	5.89	41.81	95.23	−0.045	YES	extr
CSS0042850.1	CsGRX56	CC	CYMC	133	13,931.94	4.56	43.27	115.04	0.28	NO	cyto
CSS0029842.1	CsGRL26	GRL		790	88,886.96	4.87	44.94	81.33	−0.594	NO	chlo/plas/E.R.
CSS0009287.1	CsGRX57	CGFS	CGFS	492	54,012.62	5.16	37.98	83.94	−0.274	NO	nucl
CSS0008595.1	CsGRL27	GRL		531	58,320.4	6.35	44.28	87.76	−0.235	NO	chlo
CSS0029114.1	CsGRX58	CGFS	CGFS	162	18,527.46	5.33	39.78	96.79	−0.113	NO	mito
CSS0022469.1	CsGRX59	CGFS	CGFS	167	19,075.48	5.02	31.31	73.53	−0.517	NO	nucl

3.3. Motif, Glutaredoxin Domain, and Gene Structure Analysis of CsGRXs

We performed an analysis of the conserved motifs, gene structures, and positions of glutaredoxin-conserved domains to gain a better understanding of the potential functions of CsGRX genes (Figure 3). We used the MEME online program to analyze the sequences of the 86 CsGRX proteins with a target motif maximum expectation value set to 10 to identify conserved motifs. The results showed that CsGRX members within each subtype

had similar motif patterns, but the motif patterns were different among different subtypes. Notably, both CC-type and CPYC-type motif compositions contained motif 1 and motif 2. Motif 1 was distributed to most members, except for one member in CPYC-type, five members in CGFS-type, and seven members in GRL-type. The LxxLL amino acid residues contained in motif 1 are critical for the interaction with TGA transcription factors [53], while the CCMC motif in motif 2 is one of the signature sites of CC-type (Figure 4).

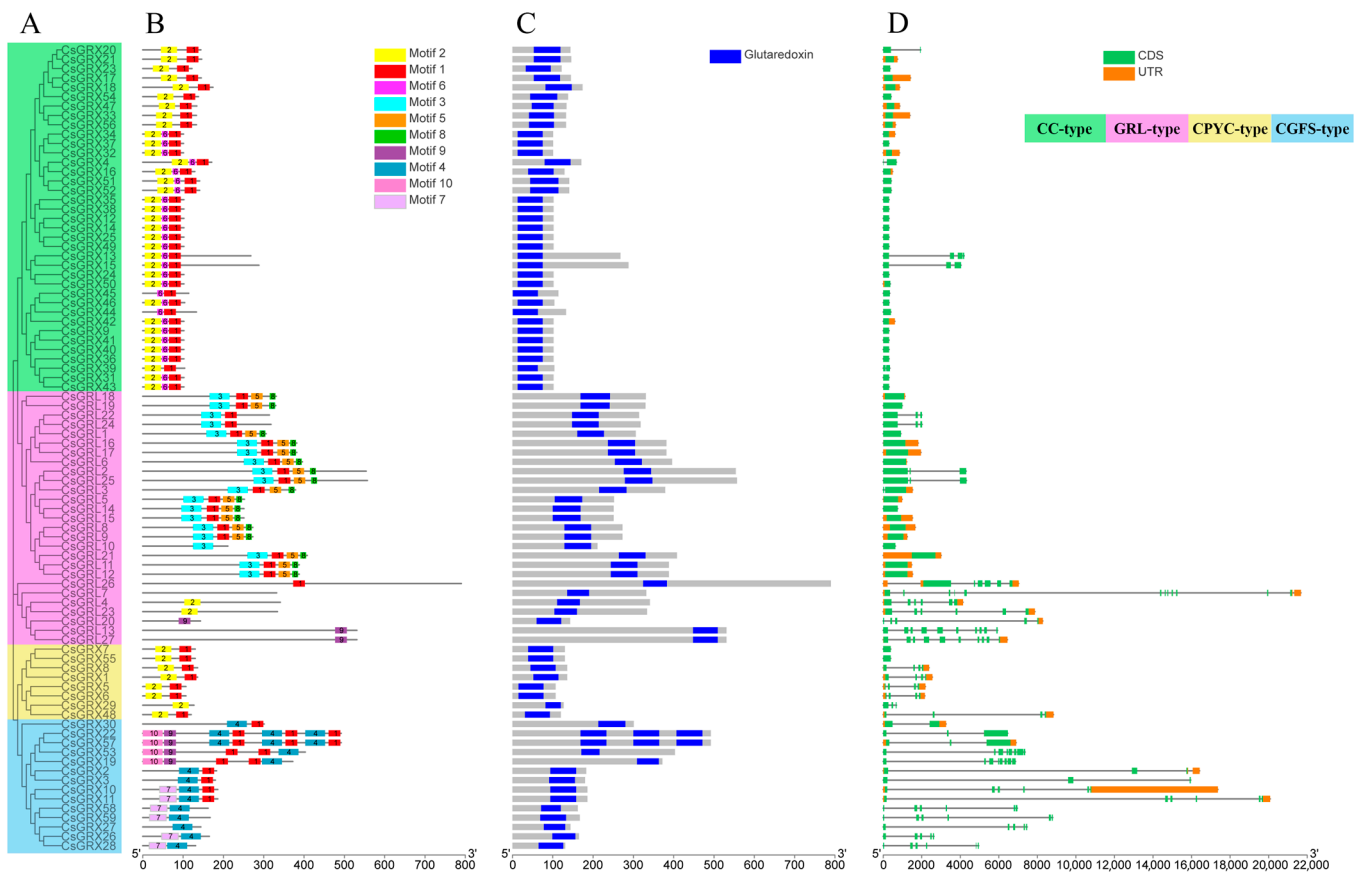


Figure 3. Phylogenetic relationships, motif compositions, conservative domains, and gene structure of the CsGRX family. (A) Eighty-six full-length CsGRX protein sequences were analyzed by MEGA X software, and the phylogenetic tree was constructed using the Neighbor-Joining (NJ) method with 1000 bootstrap reuses. (B) Each colored box represents a motif in the protein, and the motif name is displayed in the box in the upper right corner. (C) The blue box represents the position of the Glutaredoxin conserved domain, and the length can be estimated using the scale at the bottom. (D) The noncoding sequences, exons, and introns are represented by green boxes, orange boxes, and black lines, respectively.

Previous studies have shown that CC-type may have evolved from CPYC-type [55]. Based on the protein sequence and conserved motif information of CPYC-type and CC-type members in the tea GRX family, these two subtypes have very similar evolutionary status, except for the differences in conserved active sites. This is consistent with previous research and the results of phylogenetic tree analysis in this study [23]. In addition, motif 4 is only present in CGFS-type, and the CGFS motif is a hallmark of this subtype. Finally, we found that motif 3, motif 5, and motif 8 are highly abundant in GRL-type, with each containing a “CxxC[x7]CxxC” motif, similar to previous findings in Arabidopsis, rice, and poplar, suggesting this is also a hallmark of the GRL-type [23,27,56].

each contained 2~8 *CsGRX* genes. These distribution patterns suggest that the distribution of *CsGRX* genes in tea plant chromosomes is diverse.

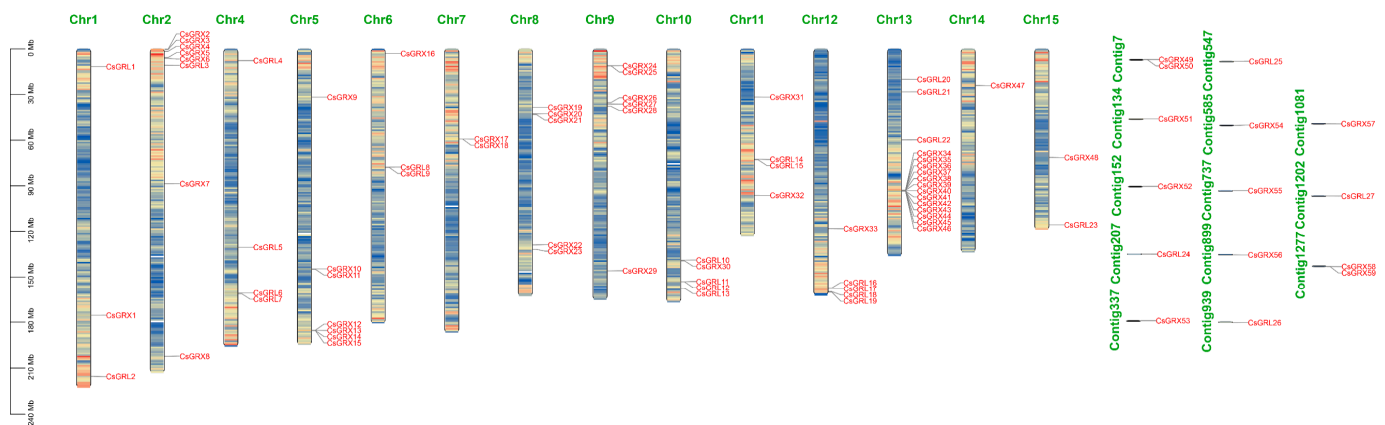


Figure 5. The chromosomal distributions of *GRX* genes in *C. sinensis* by TBtools software (v1.120). The scale on the left corresponds to chromosome length information, the filling part on the chromosome indicates the gene density at the corresponding location, the green font indicates the chromosome number, and the red font indicates the gene.

The evolution of gene families is usually accomplished by three mechanisms: whole-genome duplication, tandem duplication, and segmental duplication [61,62]. In order to study the evolutionary history of the *CsGRX* gene family in tea plants, we performed collinearity analysis on *CsGRX* genes using the MCScanX program. The results showed that there were 19 gene duplication events among the 86 *CsGRX* genes (Figure 6). Among them, *CsGRX5* and *CsGRX6* (CPYC-type) were located on the second chromosome, and their chromosomal locations were very close, indicating that these closely linked duplicate genes may have been produced by tandem duplication events. In addition, there were also two pairs of duplicated genes on the eighth chromosome, *CsGRX19* and *CsGRX22* (CGFS-type), *CsGRX21* and *CsGRX23* (CC-type); although their distances were relatively far apart, they were considered tandem duplicate genes because they belonged to the same chromosome and the same subtype. The remaining 16 pairs of duplicated genes were found to be located on different chromosomes, suggesting that they were produced by segmental duplication. These gene duplication events suggest that the *CsGRX* gene family in the tea plant may have been affected by multiple duplication mechanisms during its evolutionary process.

During the process of evolution, duplicated genes can undergo non-functionalization, sub-functionalization, or neo-functionalization [63]. In this study, 19 duplicated genes from the tea tree *GRX* gene family were selected, and their non-synonymous substitution rates (*ka*) and synonymous substitution rates (*ks*) were calculated, as well as their ratio (*Ka/Ks*) (Table 2), to infer the nature and degree of selection pressure. The magnitude of *Ka/Ks* values can be used to determine the type of selection pressure, such as *Ka/Ks* = 1 indicating neutral selection (pseudogenes), while *Ka/Ks* < 1 indicating purifying or negative selection (tendency towards purifying), and *Ka/Ks* > 1 indicating positive selection. This study found that, except for three pairs of duplicated events that could not be calculated for *Ka/Ks* values, all other gene pairs had *Ka/Ks* values less than 1, and except for *CsGRL22/CsGRL24* with *Ka/Ks* greater than 0.5, all other gene pairs had *Ka/Ks* values less than 0.5, indicating that the tea tree *GRX* gene family experienced strong purifying selection pressure during the evolution process.

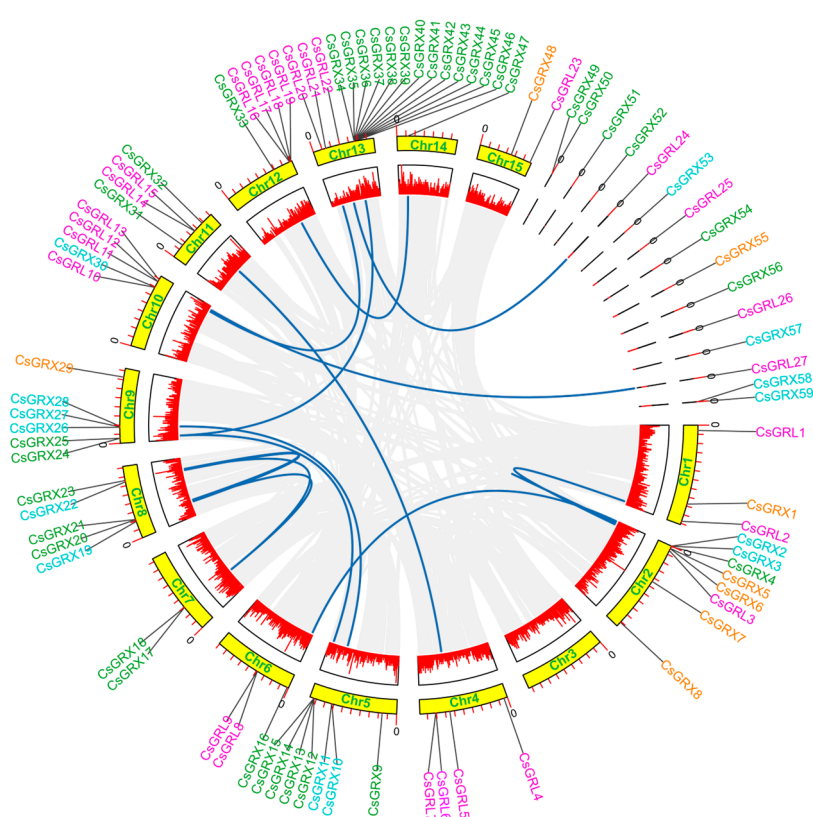


Figure 6. Syntenic relationship of duplicated gene pairs from *C. sinensis* by TBtools software (v1.120). The outermost gene and wiring indicate the approximate location of the gene on the chromosome. Yellow boxes indicate chromosomes, boxes containing red lines indicate the gene density of the corresponding chromosomes, and blue lines in the middle indicate gene duplication events.

Table 2. The evolutionary pressure of selection on the *GRX* genes in *Camellia sinensis*.

Gene_1	Gene_2	Ka	Ks	Ka/Ks
CsGRL2	CsGRL3	0.190566704	0.672904876	0.283200063
CsGRL11	CsGRL21	0.165235466	0.5242538	0.315182201
CsGRL13	CsGRL27	0.001651983	0	NaN
CsGRL15	CsGRL5	0.185775731	0.756913692	0.245438461
CsGRL14	CsGRL5	0.185775731	0.756913692	0.245438461
CsGRX33	CsGRX47	0.190034609	0.600583384	0.316416694
CsGRX34	CsGRX25	0.293717121	1.405344765	0.209000047
CsGRL22	CsGRL24	0.03704021	0.051579072	0.718124772
CsGRX5	CsGRX6	0	0.026551445	0
CsGRX4	CsGRX16	0.176674553	1.615304599	0.109375379
CsGRX14	CsGRX25	0.091802858	1.029786851	0.089147437
CsGRX15	CsGRX24	0.21162252	1.239890471	0.170678398
CsGRX11	CsGRX27	0.242722152	0.486539412	0.498874594
CsGRX12	CsGRX25	0.091802858	1.029786851	0.089147437
CsGRX13	CsGRX24	0.21110561	1.436435527	0.146964904
CsGRX17	CsGRX23	0.291354449	3.609138267	0.080726874
CsGRX17	CsGRX20	0.347882426	NaN	NaN
CsGRX19	CsGRX22	0.134788889	0.594251556	0.226821264
CsGRX21	CsGRX23	0.14346726	0.560764742	0.255842154

To further explore the potential evolutionary mechanisms of the tea tree *GRX* gene family, this study selected seven representative species, including five dicotyledonous plants (*A. thaliana*, *P. trichocarpa*, *V. vinifera*, *G. max*, and *S. lycopersicum*) and two monocotyledonous plants (*O. sativa* and *S. bicolor*), to construct inter-species collinearity maps with tea

tree (Figure 7, Table S1). The results showed that there were 115 collinear genes between tea tree and soybean, followed by poplar (89 pairs), grape (52 pairs), potato (49 pairs), and Arabidopsis (36 pairs), while only 17 and 22 collinear gene pairs were found in rice and sorghum, respectively, indicating that the collinear genes between the tea tree *GRX* gene family and dicotyledonous plants were more than those between monocotyledonous plants. From Figure 7, it can be seen that five *CsGRX* genes were marked in collinearity analysis between the tea tree and the other seven species, namely *CsGRX23*, *CsGRX32*, *CsGRL3*, *CsGRL5*, and *CsGRL15*, indicating that these genes played a key role in the evolution of the *GRX* gene family.

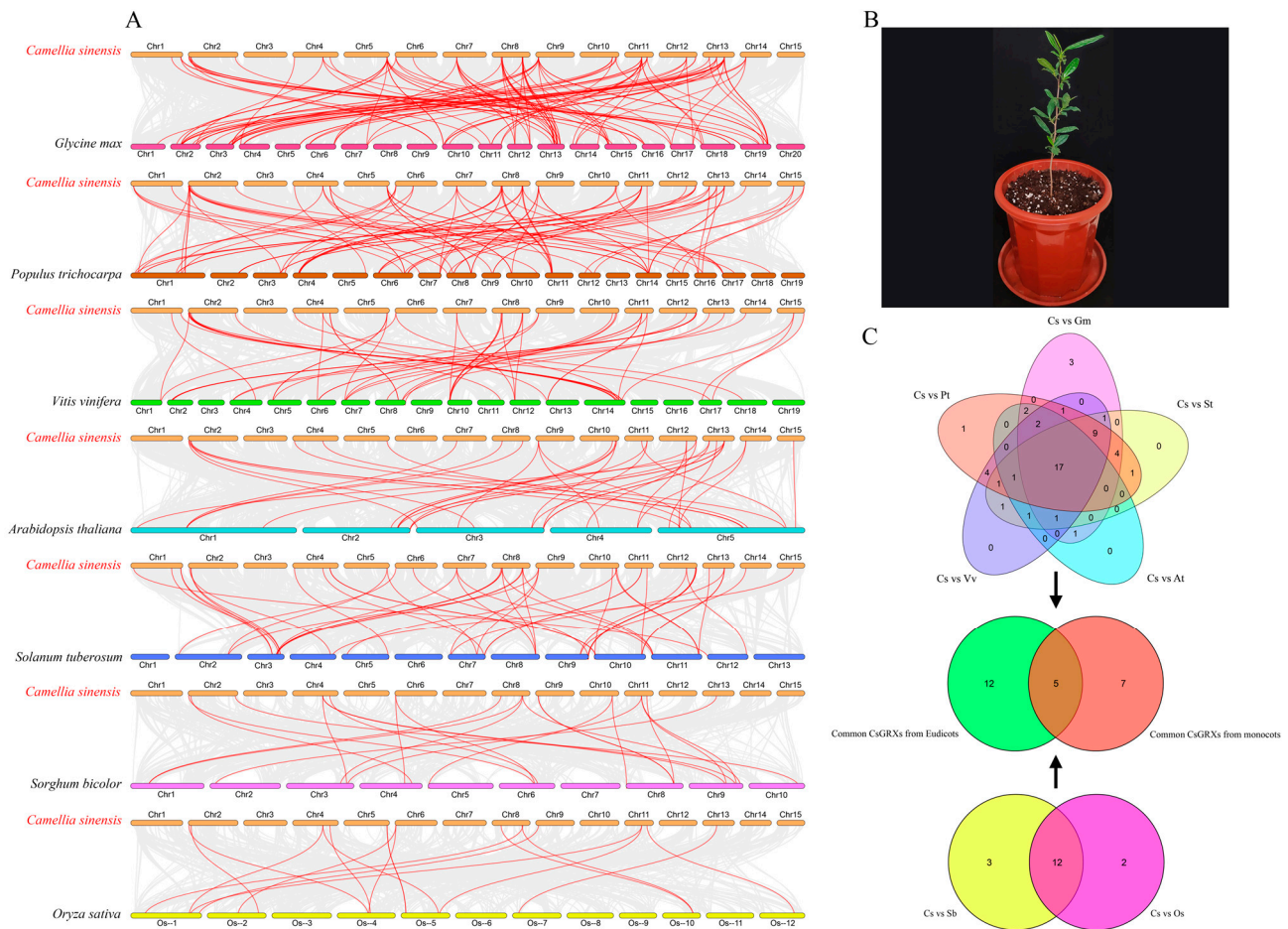


Figure 7. Collinearity analysis of *GRX* genes between *C. sinensis* and representative plants by TBtools software (v1.120). (A) Five Eudicots including *G. max* (Gm), *P. trichocarpa* (Pt), *V. vinifera* (Vv), *A. thaliana* (At), *S. tuberosum* (St); Two monocots include *O. sativa* (Os) and *S. bicolor* (Sb). (B) Physical photo of *Camellia sinensis*. (C) Collinear Venn diagram analysis of *C. sinensis* with five eudicots and two monocots.

3.5. Analysis of *CsGRXs* cis-Acting Elements in the Promoter Region

The promoter region of a gene usually contains various types of CAREs that have different roles in controlling gene expression in different tissues, developmental stages, or under environmental stresses [64,65]. In plants, various transcription factors recognize and bind to specific CAREs in the promoter region of downstream genes to finely regulate gene expression in response to biotic and abiotic stresses, thereby playing a crucial role in plant growth and development [66]. Given the importance of CAREs in response to abiotic stresses, this study extracted 2000 bp upstream of the transcription start site ATG from 86 *CsGRX* gene genomic DNA sequences and submitted them to the PlantCARE database to identify and analyze CAREs related to various stresses, growth and development, and

hormone responses in the promoter region of *CsGRX* genes. The results of the analysis, as shown in Figures 8 and 9, revealed a large number of CAREs in the promoter region of *CsGRX* genes (Figure 8, Tables S2 and S4), which were classified into four categories based on their types: (1) light response; (2) plant hormone response; (3) plant growth and development; and (4) stress response. Among them, the number of light response-related CAREs was particularly high, and they were analyzed separately. The most abundant CARE was Box 4 (28.6%), which was identified in all *CsGRX* genes except *CsGRX32*, *CsGRX50*, *CsGRX55*, *CsGRL5*, *CsGRL8*, and *CsGRL9*. In addition, light response elements such as G-box (19.2%), GT1-motif (11.5%), TCT-motif (6.8%), and GATA-motif (4.3%) were also widely identified in the promoter region of *CsGRX* genes (Figure 9).

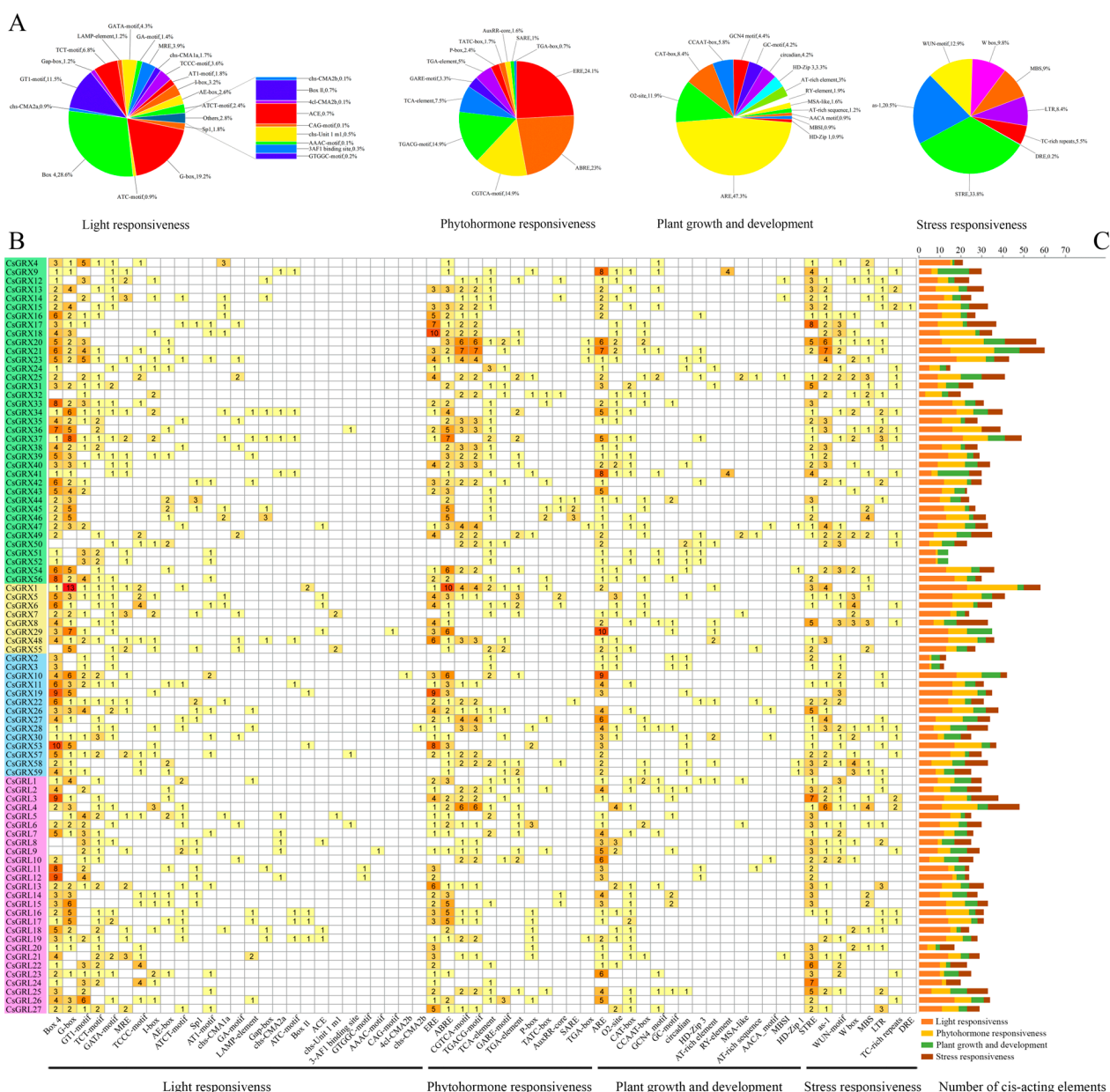


Figure 8. Statistical analysis of *cis*-acting elements in the CsGRX gene family by TBtools software (v1.120). **(A)** The proportion of all *cis*-acting elements in the CsGRX gene family in the four classifications of light responsiveness, phytohormone responsiveness, plant growth and development, and stress responsiveness. **(B)** The number and distribution of various *cis*-acting elements in each CsGRX gene. **(C)** Distribution of the four classes of *cis*-acting elements in each CsGRX gene.



Figure 9. Analysis of *cis*-acting elements in the CsGRX gene family by TBtools software (v1.120). Members of the four categories are labeled with gene IDs by different colors, and ellipses of different colors on the lines represent different types of *cis*-acting elements.

In the plant hormone response category, we identified 12 CAREs, the most common being ERE (24.1%, involved in ethylene response) and ABRE (23%, involved in abscisic acid response), followed by CGTCA-motif and TGACG-motif (14.9%, involved in MeJA-responsiveness), as well as TCA-element (7.5%, involved in salicylic acid responsiveness), TGA-element (5%, auxin-responsive element), GARE-motif (3.3%, gibberellin-responsive element), P-box (2.4%, gibberellin-responsive element), TATC-box (1.7%, involved in gibberellin-responsiveness), AuxRR-core (1.6%, involved in auxin responsiveness), SARE (1%, involved in salicylic acid responsiveness), and TGA-box (0.7%, part of an auxin-responsive element) (Figure 8).

In terms of growth and development, ARE (47.3%, *cis*-acting regulatory element essential for anaerobic induction) has the highest proportion among the plant growth and development categories. Next are O2-site (11.9%, *cis*-acting regulatory element involved in zein metabolism regulation), CAT-box (8.4%, involved in meristem expression), CCAAT-box (5.8%, MYBHv1 binding site), GCN4 motif (4.4%, involved in endosperm expression), circadian (4.2%, involved in control of circadian rhythm), and so on (Figure 8).

In the stress response category, we identified a total of 7 *cis*-acting elements related to stress, including STRE (33.8%, Pressure responsiveness), as-1 (20.5%, Disease-associated protein binding sites), WUN-motif (12.9%, wound-responsive element), W box (9.8%, WRKY transcription factor binding site involved in defense response), MBS (9%, MYB binding site involved in drought-inducibility), LTR (8.4%), TC-rich repeats (5.5%, involved in defense and stress responsiveness), and DRE (0.2%, involved in dehydration, low-temperature, and salt stresses).

3.6. Tertiary Structure Analysis of CsGRX Proteins

To understand the tertiary structure of CsGRXs, representatives from the three classic GRX subfamilies, CC-type, CGFS-type, and CPYC-type, were selected based on their homology with known protein structures in the PDB database. Homology modeling was performed using the SWISS-MODEL tool in ExPASy to generate their tertiary structure models, which were then analyzed to study the structural information of different subtypes (Figure 10). Since the tea GRL-type protein members showed no significant homology with known GRX proteins in the PDB, they were not analyzed. CsGRX25 was chosen as the representative for CC-type, and its model was built using the crystal structure of the buckwheat glutaredoxin-glutathione complex (PDB ID: I1M1D2.1.A) as a template. CsGRX5 was chosen as the representative for CPYC-type, and its model was built using the crystal structure of wheat glutaredoxin (PDB ID: A0A6A2X2B3.1.A) as a template. Similarly, CsGRX3 was chosen as the representative for CGFS-type, and its model was built using the crystal structure of Arabidopsis monothiol glutaredoxin AtGRXcp (PDB ID: 3ipz.1.A) as a template. The models included three types, and Figure 10B,C show the rotated views of Figure 10A to facilitate the observation of the labeled sites. The evaluation parameters of the models are shown in Figure S2.

From the tertiary structures of the three representative CsGRX proteins, CC-type and CPYC-type each contain six alpha helices and four beta sheets, which are the same as those in the template structures. Due to the lower homology of CGFS-type with the templates than CC-type and CPYC-type (Table S3), it contains only five alpha helices and four beta sheets, with one less alpha helix than in the templates. However, the missing third alpha helix in CsGRX3 is identical to that of the template in terms of its amino acid residues, consisting of only three amino acids. This suggests that the overall structure of the tea GRX gene is conserved. Three conserved regions are marked in Figure 10A, including the conserved active site of the GRX gene marked in red and the blue sites involved in GSH binding, which are the highly conserved TVP and the less conserved CDD amino acid sequences [67]. Previous studies have shown that the GSH binding site contains lysine near the first beta-sheet and glutamic acid near the third alpha helix, in addition to the three signature sites labeled here. GSH binds to the conserved GSH binding site of GRX through

hydrogen bonding, salt bridges, and hydrophobic interactions, playing a role as a scaffold protein and transporting GSH [68].

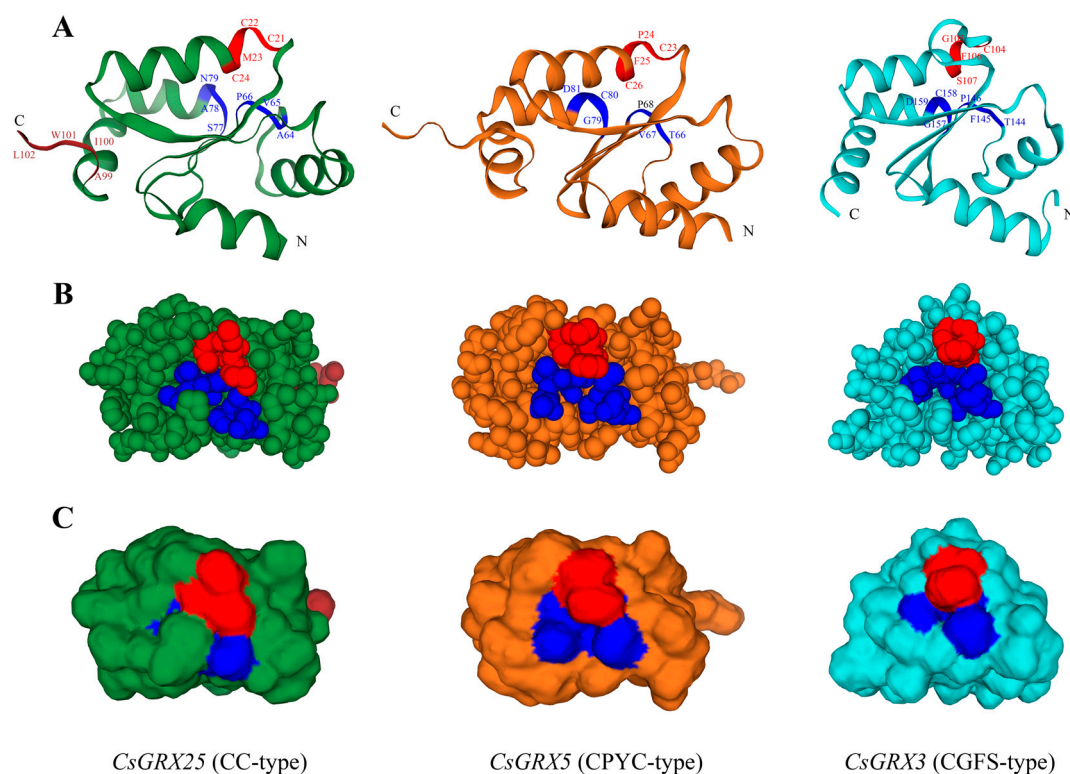


Figure 10. Structure of representative CPYC-type, CGFS-type, and CC-type GRX proteins from *C. sinensis* by SWISS-MODEL program. (A) Predictive structure of CsGRX25, CsGRX5 and CsGRX3. Residues of GSH binding sites are color-coded. (B,C) Surface structures of CsGRX25, CsGRX5, and CsGRX3.

3.7. Gene Ontology Analysis and Protein–Protein Interaction (PPI) Network Prediction

For functional analysis of the tea tree GRX gene family, GO enrichment analysis revealed that most CsGRXs were enriched in processes such as reactive oxygen species metabolism, stress response, and ion binding and were mainly concentrated in the plasma membrane, cell periphery, chloroplast stroma, and plastid stroma in Cellular component analysis. Through KEGG enrichment analysis, most CsGRX genes were found to be enriched in pathways such as Chaperones and folding catalysts, Protein families: genetic information processing, Protein phosphatases and associated proteins, and Brite Hierarchies. These results can further help us understand the mechanism and function of CsGRX genes in response to various stress stimuli in tea trees (Figure 11).

Protein–protein interaction (PPI) analysis is an important method for studying the relationships between proteins. It can help understand the interactions between proteins and their roles in cellular processes. By analyzing the connections in the network, it is possible to reveal the interactions between different proteins [69]. In this study, a PPI network for the tea plant GRX family was constructed using the STRING database, with a total of 79 members involved in network construction (Figure 12). From the network, it is clear that CsGRX3, CsGRL27, and CsGRX30 have the closest interactions with other members, indicating that they may be key members involved in responding to oxidative stress and maintaining cellular homeostasis. In addition, CsGRX proteins have multiple functional partners, including glutathione reductase (GR), 2-Cys Peroxiredoxin BAS1, TGA3, THX, SRX, and others. These interacting proteins are of great significance for further studying the roles of CsGRXs in response to various stress conditions in tea plants.



Figure 11. Gene ontology (GO) analysis and Kyoto Encyclopedia of Genes and Genomes (KEGG) analysis of CsGRX genes. The redder the color of the bubble in (A,C) indicates higher significance, and the larger the bubble indicates the greater number of genes enriched into the item. (B,D) represent specific entries of CsGRX genes in GO and KEGG enrichment analysis, respectively.

3.8. Transcriptional Analysis of GRX Genes in Multiple Tissues

To gain a deeper understanding of the expression patterns of CsGRX genes in tea plant growth and development, we obtained the expression profiles of tea plant GRX genes in different tissues, including stem, apical bud, young leaf, mature leaf, old leaf, flower, fruit, and root. The heatmap based on gene expression levels clearly showed the differential expression of CsGRX genes among different tissues (Figure 13, Table S7). Among the 86 CsGRX members, 19 members had low expression in all eight tissues, with an average FPKM < 1. Members of different subtypes showed expression preferences in different tissues. Members of the CC-type were induced the most in roots, flowers, and fruits, with CsGRX17 and CsGRX18 showing the highest relative expression levels in roots and CsGRX47 showing high expression in flowers. Members of the GRL-type were mainly expressed in three types of leaves. Interestingly, members of the CPYC-type and CGFS-type subtypes showed little difference in expression levels across the eight tissues.

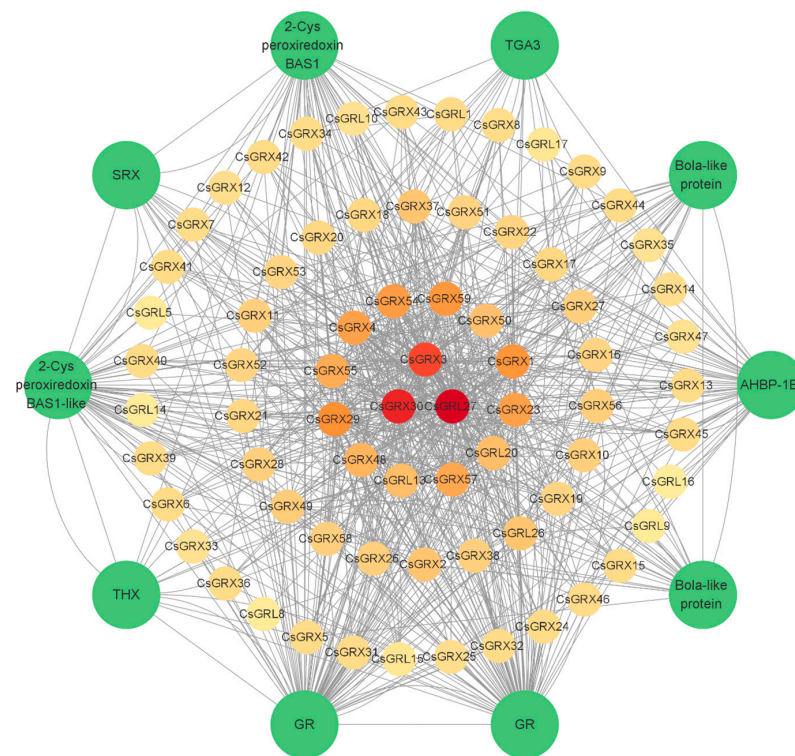


Figure 12. The protein–protein interaction (PPI) network analysis of CsGRX proteins was visualized with Cytoscape software (v3.9.1). The middle orange nodes represent the CsGRX proteins, and the outer ten green nodes are predicted proteins that interact with CsGRXs.

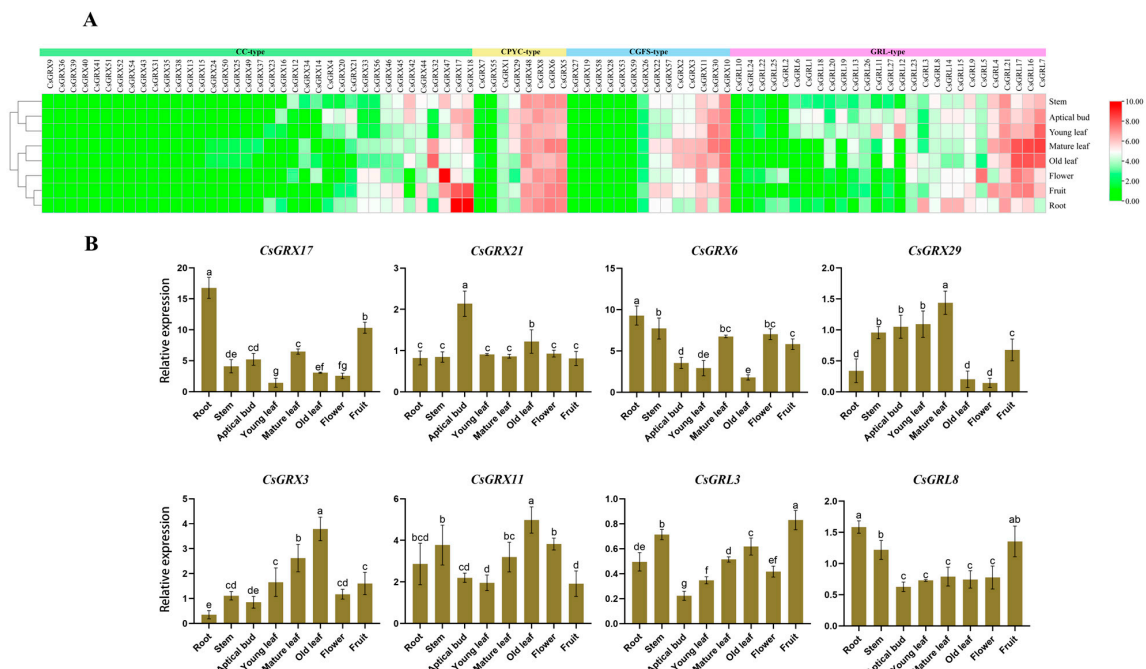


Figure 13. Expression pattern of CsGRX genes. **(A)** Expression analysis of CsGRX genes in different tissues based on RPKM values. The red and green colors represent high and low expression levels, respectively. **(B)** The expression levels of selected CsGRX genes in eight different tissues (stem, apical bud, young leaf, mature leaf, old leaf, flower, fruit, and root) were confirmed by RT-qPCR. The error bars represent the standard deviation of three independent biological replicates. Letters with the same label indicate no significant difference at $p < 0.05$ by Duncan's multiple range test.

In addition, the RT-qPCR results revealed tissue-specific expression patterns of CsGRX genes with varying expression levels, consistent with the transcriptomic data (Figure 13B). Among them, CsGRX21 and CsGRL8 exhibited relatively stable expression across all tissues, while the other six members showed high expression in the roots, except for CsGRX29 and CsGRX3. CsGRX17 exhibited the highest expression level in the roots, CsGRX21 showed high expression in the apical bud, and CsGRX29 displayed the lowest expression levels in the old leaf and flower tissues.

Overall, the differential expression patterns of CsGRX genes in different tissues suggest that different members play distinct roles in the growth and development of tea plants.

3.9. Expression Patterns of CsGRXs Genes under Drought and Cold Stresses

During growth and development, tea plants often encounter various abiotic stresses. In order to gain insight into the role of CsGRX genes under stress conditions, we retrieved and visualized the expression profiles of tea plant GRX genes under drought and cold stress from the TPIA database. The analysis results showed that more than half of the CsGRX genes did not show significant differential expression under stress conditions (Figure 14, Tables S5 and S6). Under drought stress, the expression levels of CsGRX17, CsGRX18, and CsGRX47 in the CC-type decreased significantly, while the expression levels of CsGRX42, CsGRX21, CsGRX20, CsGRX37, and CsGRX23 increased significantly. In the CPYC-type, the expression levels of CsGRX29 and CsGRX6 decreased significantly, and no genes showed significant up-regulation. In the CGFS-type, the expression levels of CsGRX2, CsGRX3, CsGRX11, and CsGRX10 were down-regulated, while the expression level of CsGRX26 was up-regulated. In addition, the GRL-type showed the most differentially expressed genes, with up-regulated genes including CsGRL22, CsGRL24, CsGRL1, CsGRL26, CsGRL23, and CsGRL8, and down-regulated genes including CsGRL13, CsGRL20, CsGRL27, CsGRL4, CsGRL3, and CsGRL17. It is worth noting that some members of the GRL-type showed an initial increase followed by a decrease in expression level, such as CsGRL25 and CsGRL2. Additionally, many CsGRX genes also responded to cold stress, exhibiting differential expression during cold treatment (Figure 14B). In fact, the expression levels of most differentially expressed genes were up-regulated under cold stress at different time points, with members mainly concentrated in the CC-type, such as CsGRX20, CsGRX34, CsGRX17, and CsGRX18. In addition, both the CGFS-type and GRL-type were sensitive to cold stress, such as CsGRX11 and CsGRL23. It is worth noting that although these genes were all up-regulated under cold stress, their response times were different. For example, the expression levels of CsGRX17 and CsGRX18 significantly increased at 6 h and decreased at 7 d, while genes such as CsGRX11 and CsGRL23 showed a continuous increase in expression levels under cold stress without a downward trend. Moreover, almost all differentially expressed genes showed a significant decrease in expression levels after domestication.

We also analyzed the response of representative CsGRX genes to drought stress using RT-qPCR. Their expression levels in roots and leaves were determined at 0, 1, 3, 6, 12, 24, 48, and 72 h after treatment with 20% PEG-6000. The results are shown in Figure 15. In leaf tissues, the target genes CsGRX6, CsGRX29, CsGRX3, and CsGRL3 were up-regulated in response to drought at different time points, with a 2-fold increase compared to 0 h at 72 h. However, in roots, a greater number of CsGRX genes were induced by PEG-6000, except for CsGRL3, with the remaining seven members showing upregulation. CsGRX17, CsGRX21, CsGRX11, and CsGRL8 reached their peak expression at 6 h. This indicates organ-specific regulation of CsGRX genes under drought conditions.

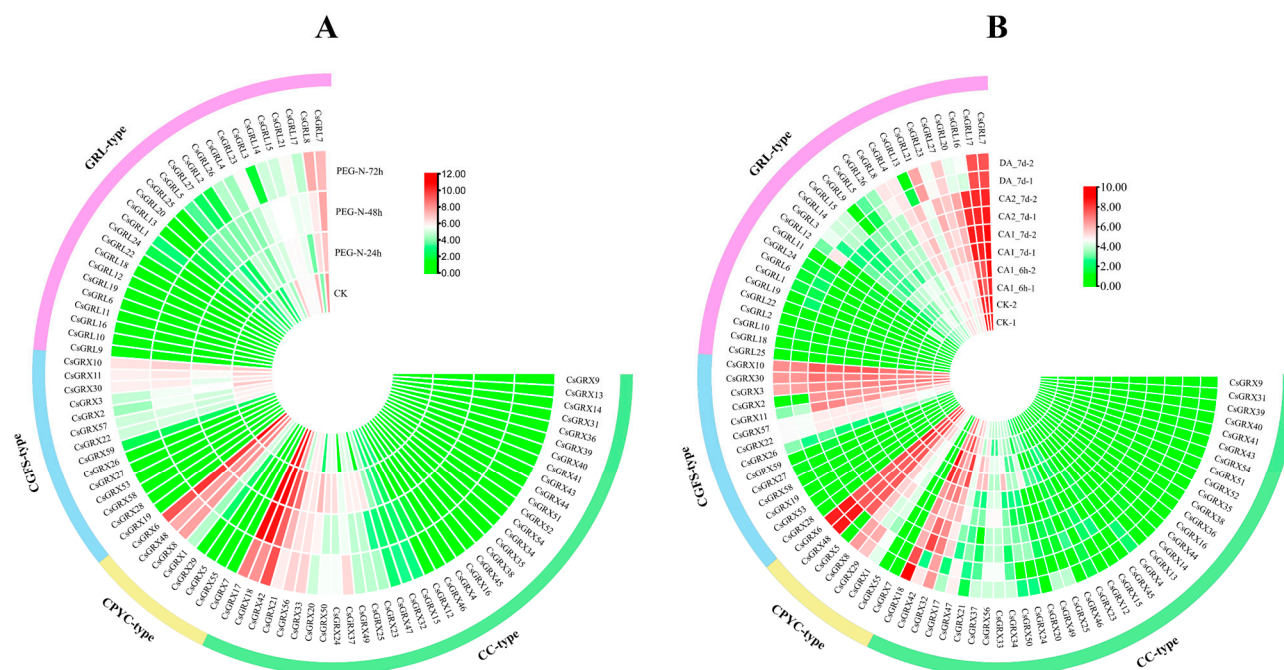


Figure 14. Expression patterns of CsGRX genes under drought and cold stresses. (A) The expression patterns of CsGRX genes in response to 25% PEG treatment for 0, 24, 48 and 72 h. (B) The expression patterns of CsGRX genes in response to cold acclimation. The five stages represent non-acclimated at 25–20 °C (CK-1, CK-2), fully acclimated at 10 °C for 6 h (CA1_6h-1, CA1_6h-2), and 10–4 °C for 7 days (CA1_7d-1, CA1_7d-2), cold response at 4–0 °C for 7 days (CA2_7d-1, CA2_7d-2), and recovering under 25–20 °C for 7 days (DA_7d-1, DA_7d-2).

3.10. RT-qPCR Analysis of Representative CsGRXs under Salt Stress

RT-qPCR was employed to analyze the expression patterns of CsGRX genes under salt stress conditions (100 mM NaCl). The expression levels of eight representative CsGRX genes, representing CC-type, CPYC-type, CGFS-type, and GRL-type, were recorded at 0, 1, 3, 6, 12, 24, 48, and 72 h after treatment. Figure 16 illustrates the fold induction of CsGRX genes in NaCl-treated samples relative to untreated samples. In leaf tissue, CsGRX17 and CsGRX21 were up-regulated at 6 h and 48 h, while they were suppressed at 72 h. CsGRX29 and CsGRL8 exhibited similar expression patterns, showing an overall upward trend under salt conditions. All eight tested members displayed distinct differential expression levels. In roots, CsGRX17, CsGRX21, CsGRX6, and CsGRX11 showed similar expression patterns, decreasing to control levels by 72 h. CsGRX3 and CsGRL3 peaked at 6 h but continued to exhibit an upward trend at 72 h. Overall, these results indicate that CsGRX gene members exhibit differential sensitivity to salt treatment.

3.11. Differential Expression Patterns of Representative CsGRXs after SA Treatment

The expression patterns of CsGRX genes after salicylic acid (SA) treatment were also analyzed using RT-qPCR. The relative expression levels of eight representative CsGRX genes were recorded at 0, 1, 3, 6, 12, 24, 48, and 72 h after SA treatment (Figure 17). In leaf tissue, CsGRX17 and CsGRX29 reached their highest expression levels at 12 h, showing 3.18-fold and 2.38-fold increases, respectively, compared to the 0 h samples. CsGRX6, CsGRL3, and CsGRL8 were up-regulated under SA induction and displayed similar expression patterns. On the other hand, CsGRX11 initially downregulated and then up-regulated after SA treatment, reaching the lowest expression level at 12 h. In the root tissue, CsGRX21, CsGRX6, and CsGRX11 exhibited similar expression patterns, peaking around 12 h. CsGRX17 showed the highest expression level at 24 h, CsGRX29 peaked at 3 h, and CsGRL8 reached its maximum expression level at 48 h. Compared to leaf tissue, except for CsGRX11, which showed an opposite expression pattern, there were

no significant differences in the expression patterns among the other members, indicating that the organ-specific expression of *CsGRX* genes was not apparent under SA treatment. Overall, exogenous SA hormone induced the expression of *CsGRX* genes.

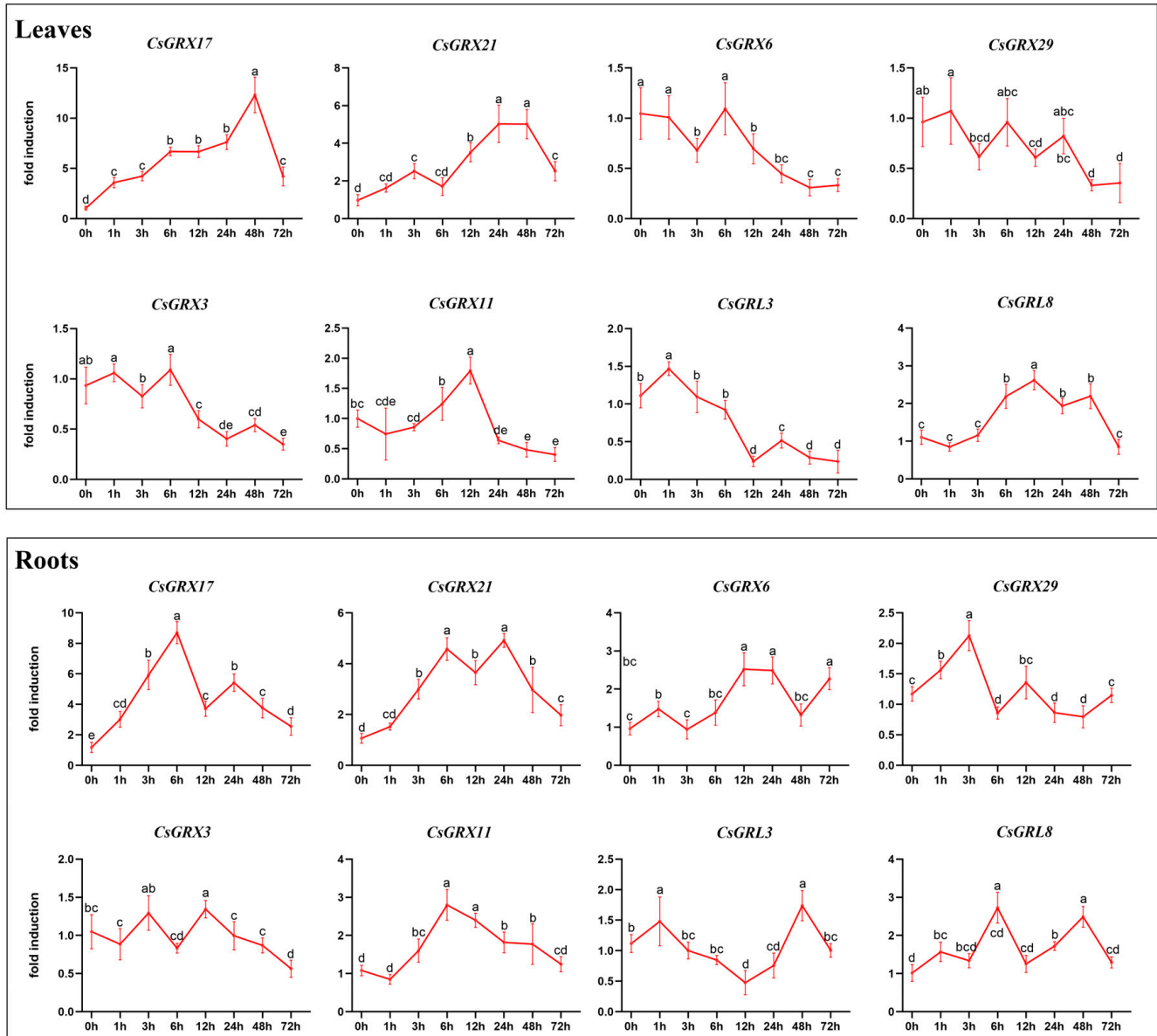


Figure 15. Expression levels of representative *CsGRX* genes under drought conditions. Plants were treated with 20% PEG-6000, and roots and leaves were harvested at 0, 1, 3, 6, 12, 24, 48, and 72 h for total RNA extraction and RT-qPCR analysis. The *GAPDH* gene was used as an internal control, and the relative gene expression was calculated using the $2^{-\Delta\Delta CT}$ method. The relative expression values of each gene compared to the internal control gene in the untreated control samples were set to 1. The data presented are the average values of three biological replicates. The different letters indicate significant differences determined by Duncan's multiple range test at $p < 0.05$.

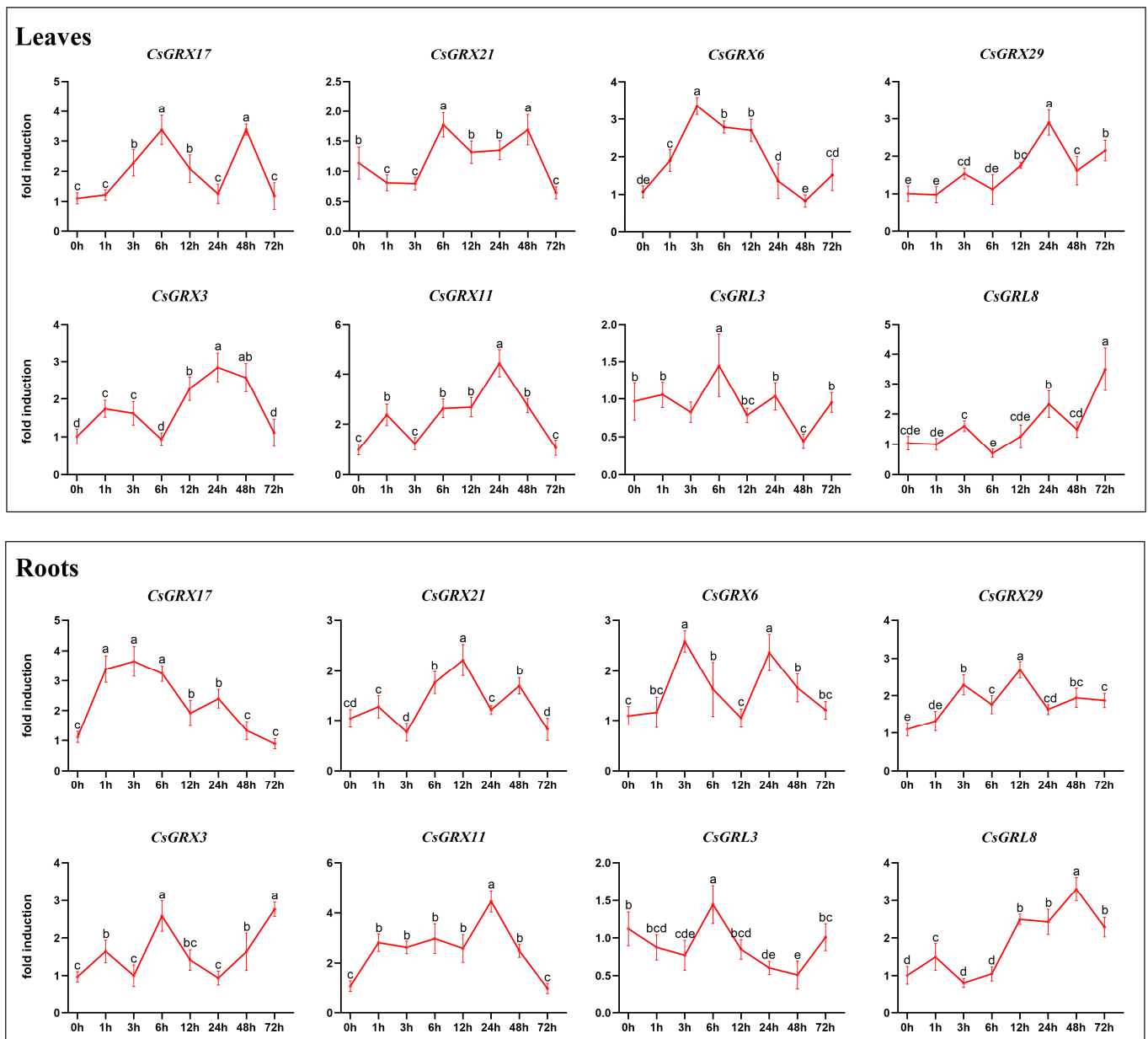


Figure 16. Expression profiles of representative *CsGRX* genes in response to salt stress. Plants were treated with NaCl (100 mM), and root and leaf samples were collected at 0, 1, 3, 6, 12, 24, 48, and 72 h for total RNA extraction and RT-qPCR analysis. *GAPDH* was used as the reference gene, and relative expression was calculated using the $2^{-\Delta\Delta CT}$ method. The relative expression values of each gene compared to the reference gene in the untreated control samples were set to 1. Data represent the average of three biological replicates. The different letters indicate significant differences determined by Duncan's multiple range test at $p < 0.05$.

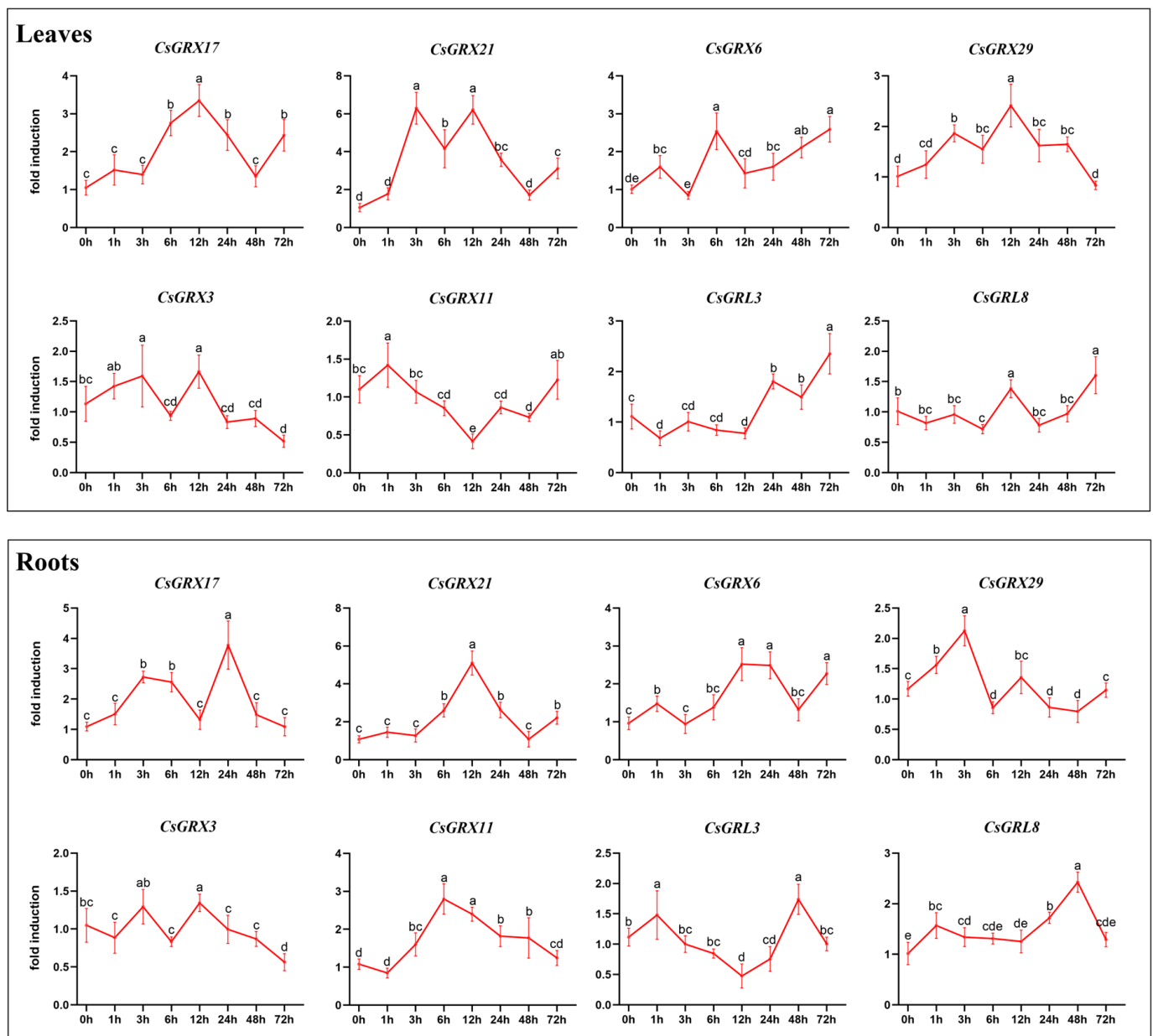


Figure 17. The expression levels of representative *CsGRX* genes after salicylic acid (SA) treatment. Plants were treated with SA, and samples of roots and leaves were collected at 0, 1, 3, 6, 12, 24, 48, and 72 h for total RNA extraction and RT-qPCR analysis. The *GAPDH* gene was used as an internal control, and relative gene expression was calculated using the $2^{-\Delta\Delta CT}$ method. The relative expression values of each gene compared to the untreated control samples were set to 1. The data presented are the average values of three independent biological replicates. The different letters indicate significant differences determined by Duncan's multiple range test at $p < 0.05$.

4. Discussion

Currently, the *GRX* gene family has been identified and analyzed in various plants, and members have been found to play critical roles in plant physiological development [23–27]. However, in tea plants, the *GRX* gene family has not been systematically analyzed. In this study, we identified 86 *CsGRX* genes in the tea plant genome using two methods, BLAST and HMMER, and confirmed the existence of the *GRX* domain in the encoded proteins of these genes through the InterPro and SMART databases. Based on the conservation of the oxidative-reductive active sites and phylogenetic analysis of these genes, we classified *CsGRX* proteins into four subtypes: CC-type, CPYC-type, CGFS-type, and GRL-type. CC-

type is the most abundant subtype among the typical GRX subtypes (37 in total), which is consistent with previous research in cassava and maize [28,70]. Notably, previous studies have shown that CC-type is a subtype unique to plants and has only been identified in plants [29,30,71]. The significant increase in the number of CC-type genes has contributed to the evolution of plant-specific functions to cope with various unavoidable environmental stresses [29]. We identified 27 GRL-type members in tea plants. GRL-type members do not share the primary conserved oxidative-reductive active site but display four conserved CxxC motifs arranged in the form of “CxxC[x7]CxxC” at the C-terminal end of the protein sequence [23,27,56]. Phylogenetic analysis showed that the GRL-type has lower homology than the other three classical GRX subtypes, which is similar to the GRL-type structure reported in Arabidopsis, rice, and poplar [23]. In addition, the number of CC-type and GRL-type members is much higher than that of CPYC-type and CGFS-type, which is consistent with previous research results [26,27]. Further analysis based on sequence alignment, gene structure, and conserved motifs supported the above four classifications. As shown in Figure 3, the number of exons-introns, conserved motifs, and conserved oxidative-reductive active sites of members of the same subtype is highly conserved, but there are significant differences between different subtypes. This suggests that gene recombination may occur within the same subtype, such as gaining/losing exons/introns and inserting/deleting them, which plays an important role in expanding the *CsGRX* gene family members. Compared with the *GRX* family in Arabidopsis (48) and rice (48), the number of *GRXs* in tea plants is higher. It is well known that gene replication events may lead to non-functionalization, sub-functionalization, and neo-functionalization of genes [72]. The tea plant *GRX* gene family members underwent tandem duplication and fragment replication events during evolution, which is one of the reasons for the differences in the number of *GRXs* among different plant species. The number of identified *GRX* genes in tea plants and two monocots is significantly lower than that in eudicots, indicating that the differentiation of *GRX* genes in eudicots and monocots occurred rapidly. In addition, five *GRX* genes exhibit syntenic relationships among tea and all seven species, indicating that these *GRXs* were present before the differentiation of dicotyledonous and monocotyledonous plants. Four subtypes of the *GRX* gene family are widely distributed in plants, suggesting that gene duplication and diversification may have occurred prior to the differentiation of dicotyledonous and monocotyledonous plants. Selection pressure analyses of homologous *CsGRX* genes indicate that all known 16 gene pairs have a K_a/K_s ratio less than 1, and 15 pairs have a K_a/K_s ratio less than 0.5, indicating that *CsGRX* genes have undergone strict purifying selection to preserve their original functions during long-term evolutionary processes. Subcellular localization predictions have significant implications for further studies on gene function. In this study, *CsGRX* genes located in the chloroplast, cytoplasm, nucleus, and mitochondria accounted for 82.6% of the total number, with 11.6% located in the nucleus, including four CC-type members. There was an article reported that *GRX* genes could potentially be localized in all cellular components except the nucleus [17]. However, it was shown that some CC-type members were nuclear-localized and played a significant role in the initiation and further morphogenesis of petals [73,74]. On the other hand, several *cis*-elements related to growth and development, phytohormone responses, and stress responses were detected in *CsGRX* promoter region, indicating that *CsGRXs* are regulated by a variety of plant hormones in addition to be involved in various stress responses. Furthermore, light-responsive elements were identified in all *CsGRX* promoters, indicating that *CsGRX* is sensitive to changes in light conditions and plays a crucial role in photosynthesis and other light-dependent physiological processes [75].

Plants are subjected to various environmental stressors during their growth and development, and they have evolved various defense mechanisms to cope with these stressors [76]. Gene expression profiling is an important approach to studying gene function, and extensive studies have demonstrated that *GRX* genes play a mitigating role in excess ROS generated by plants in response to various stressors. In this study, the expression of *CsGRX* genes was induced under multiple abiotic stresses, and *CsGRX17*, *CsGRX18*,

CsGRX48, *CsGRX6*, *CsGRX30*, *CsGRX10*, *CsGRL17*, and *CsGRL7* were highly expressed under drought and cold stress, a large number of *CsGRX* members were also induced to express under SA treatment suggesting that these members may play a critical role in response to abiotic stress. Similarly, it has been reported that *GRX* genes are essential in response to abiotic stress in various plants, with the overexpression of *LOC_Os02g40500* and *LOC_Os01g27140* in rice significantly improving its drought tolerance [77], the expression of *AtGRXS17* in *Arabidopsis* conferring drought tolerance in tomato [78], and CC-type members in cassava induced by drought stress [70]. Additionally, a study has confirmed that Chickpea *GRX* genes provide tolerance to salinity and drought [79]. In conclusion, the differential expression of *GRX* genes indicates that they may be involved in various abiotic stress responses, playing a critical role in maintaining the organism's redox homeostasis.

5. Conclusions

This study conducted a comprehensive genomic-wide analysis of the *glutaredoxin* (*GRX*) gene family in tea plants. A total of 86 *CsGRX* genes were identified based on the glutaredoxin domain, which was divided into four subtypes: CC-type, CPYC-type, CGFS-type, and GRL-type, according to phylogenetic and conserved motif structures. Chromosomal localization and gene collinearity analysis showed that the tea plant *GRX* gene family had undergone tandem and segmental duplications during evolution, which were important ways for the expansion of *CsGRX* family members. To maintain the original function of *GRX* genes, the tea plant *GRX* gene family underwent purification selection. In addition, we provided detailed results of subcellular localization prediction, conserved motif analysis, and gene structure analysis of *CsGRX* genes and their coding proteins. Promoter *cis*-acting element analysis showed that *CsGRX* genes contained a large number of regulator elements, including those involved in plant growth and development, hormone response, and stress response. The three-dimensional structure of *CsGRX* proteins predicted by machine learning demonstrated the mechanism of interaction with the GSH co-factor. The protein–protein interaction network constructed based on the predicted interaction partners of *CsGRX* proteins and enrichment analysis confirmed their important role in oxidative-reductive reactions. Differential expression of *CsGRX* genes under different stresses indicated that their expression was induced by various abiotic stresses. Moreover, differential expression in different tissues suggested functional diversities among *CsGRX* genes. Overall, this study provides a comprehensive bioinformatics analysis and basic functional analysis of the tea plant *GRX* gene family, which provides useful information for the study of tea plant stress resistance and the breeding of high-quality tea varieties.

Supplementary Materials: The following supporting information can be downloaded at: <https://www.mdpi.com/article/10.3390/f14081647/s1>, Figure S1: Predicted subcellular localization distribution of 86 *CsGRX* proteins; Figure S2: Ramachandran Plot of a tertiary structural model of three representative *GRX* proteins of tea plant. A, B, and C represent the Ramachandran Plot and related parameters of *CsGRX25*, *CsGRX5* and *CsGRX3*, respectively; Table S1: Orthologous relationships of *GRX* genes between *Camellia sinensis* and seven representative plants (*Glycine max*, *Populus trichocarpa*, *Vitis vinifera*, *Arabidopsis thaliana*, *Solanum tuberosum*, *Oryza sativa*, and *Sorghum bicolor*); Table S2: The location information of *cis*-regulatory elements in the *CsGRXs* promoter region; Table S3: Protein 3D model matching parameters for three representative *CsGRX* genes; Table S4: The number of *cis*-regulatory elements in the *CsGRXs* promoter region; Table S5: Expression profile (FPKM value) of *CsGRX* genes under cold stress; Table S6: Expression profile (FPKM value) of *CsGRX* genes under drought stress; Table S7: Expression profile (FPKM value) of *CsGRX* genes in 8 tissues; Table S8: Information on conservative motifs in *CsGRXs*; Table S9: Primers used in this study.

Author Contributions: L.-J.H., N.L., S.D., D.J. and Y.L.: Conceptualization. D.J. and G.Y.: Data curation. D.J., W.Y. and G.Y.: Investigation. W.Y. and N.L.: Resources. J.P. and N.L.: Funding acquisition. J.P., S.D. and Y.L.: Supervision. L.-J.H. and N.L.: Methodology. D.J. and L.-J.H.: Writing—original draft, Writing—review and editing. All authors have read and agreed to the published version of the manuscript.

Funding: This work was supported by the Education Department of Hunan Province (20A392 and 20A517), the Training Program for Excellent Young Innovators of Changsha (kq2009016), and the Natural Science Foundation of Hunan Province (2020JJ5970 and 2021JJ31141).

Data Availability Statement: Not applicable.

Conflicts of Interest: The authors declare no conflict of interest.

References

1. Møller, I.M.; Jensen, P.E.; Hansson, A. Oxidative Modifications to Cellular Components in Plants. *Annu. Rev. Plant Biol.* **2007**, *58*, 459–481. [[CrossRef](#)] [[PubMed](#)]
2. You, J.; Chan, Z. ROS Regulation during Abiotic Stress Responses in Crop Plants. *Front. Plant Sci.* **2015**, *6*, 1092. [[CrossRef](#)] [[PubMed](#)]
3. Zhu, J.-K. Abiotic Stress Signaling and Responses in Plants. *Cell* **2016**, *167*, 313–324. [[CrossRef](#)] [[PubMed](#)]
4. Choudhury, F.K.; Rivero, R.M.; Blumwald, E.; Mittler, R. Reactive Oxygen Species, Abiotic Stress and Stress Combination. *Plant J.* **2017**, *90*, 856–867. [[CrossRef](#)] [[PubMed](#)]
5. Ning, X.; Sun, Y.; Wang, C.; Zhang, W.; Sun, M.; Hu, H.; Liu, J.; Yang, L. A Rice CPYC-Type Glutaredoxin OsGRX20 in Protection against Bacterial Blight, Methyl Viologen and Salt Stresses. *Front. Plant Sci.* **2018**, *9*, 111. [[CrossRef](#)]
6. Hossain, M.A.; Bhattacharjee, S.; Armin, S.-M.; Qian, P.; Xin, W.; Li, H.-Y.; Burritt, D.J.; Fujita, M.; Tran, L.-S.P. Hydrogen Peroxide Priming Modulates Abiotic Oxidative Stress Tolerance: Insights from ROS Detoxification and Scavenging. *Front. Plant Sci.* **2015**, *6*, 420. [[CrossRef](#)]
7. Huang, H.; Ullah, F.; Zhou, D.-X.; Yi, M.; Zhao, Y. Mechanisms of ROS Regulation of Plant Development and Stress Responses. *Front. Plant Sci.* **2019**, *10*, 800. [[CrossRef](#)]
8. Mondal, S.; Kumar, V.; Singh, S.P. Phylogenetic Distribution and Structural Analyses of Cyanobacterial Glutaredoxins (Grxs). *Comput. Biol. Chem.* **2020**, *84*, 107141. [[CrossRef](#)]
9. Noctor, G.; Mhamdi, A.; Foyer, C.H. The Roles of Reactive Oxygen Metabolism in Drought: Not so Cut and Dried. *Plant Physiol.* **2014**, *164*, 1636–1648. [[CrossRef](#)]
10. Meyer, Y.; Belin, C.; Delorme-Hinoux, V.; Reichheld, J.-P.; Riondet, C. Thioredoxin and Glutaredoxin Systems in Plants: Molecular Mechanisms, Crosstalks, and Functional Significance. *Antioxid. Redox Signal.* **2012**, *17*, 1124–1160. [[CrossRef](#)]
11. Fernandes, A.P.; Holmgren, A. Glutaredoxins: Glutathione-Dependent Redox Enzymes with Functions Far beyond a Simple Thioredoxin Backup System. *Antioxid. Redox Signal.* **2004**, *6*, 63–74. [[CrossRef](#)] [[PubMed](#)]
12. Ouyang, Y.; Peng, Y.; Li, J.; Holmgren, A.; Lu, J. Modulation of Thiol-Dependent Redox System by Metal Ions via Thioredoxin and Glutaredoxin Systems. *Metallomics* **2018**, *10*, 218–228. [[CrossRef](#)] [[PubMed](#)]
13. Cao, Y.; Jiang, G.; Li, M.; Fang, X.; Zhu, D.; Qiu, W.; Zhu, J.; Yu, D.; Xu, Y.; Zhong, Z.; et al. Glutaredoxins Play an Important Role in the Redox Homeostasis and Symbiotic Capacity of Azorhizobium Caulinodans ORS571. *Mol. Plant Microbe Interact.* **2020**, *33*, 1381–1393. [[CrossRef](#)]
14. Ogata, F.T.; Branco, V.; Vale, F.F.; Coppo, L. Glutaredoxin: Discovery, Redox Defense and Much More. *Redox Biol.* **2021**, *43*, 101975. [[CrossRef](#)]
15. Gallogly, M.M.; Starke, D.W.; Mieyal, J.J. Mechanistic and Kinetic Details of Catalysis of Thiol-Disulfide Exchange by Glutaredoxins and Potential Mechanisms of Regulation. *Antioxid. Redox Signal* **2009**, *11*, 1059–1081. [[CrossRef](#)] [[PubMed](#)]
16. Ukuwela, A.A.; Bush, A.I.; Wedd, A.G.; Xiao, Z. Reduction Potentials of Protein Disulfides and Catalysis of Glutathionylation and Deglutathionylation by Glutaredoxin Enzymes. *Biochem. J.* **2017**, *474*, 3799–3815. [[CrossRef](#)]
17. Rouhier, N.; Gelhaye, E.; Jacquot, J.-P. Plant Glutaredoxins: Still Mysterious Reducing Systems. *Cell Mol. Life Sci.* **2004**, *61*, 1266–1277. [[CrossRef](#)]
18. Rouhier, N.; Lemaire, S.D.; Jacquot, J.-P. The Role of Glutathione in Photosynthetic Organisms: Emerging Functions for Glutaredoxins and Glutathionylation. *Annu. Rev. Plant Biol.* **2008**, *59*, 143–166. [[CrossRef](#)]
19. Daniel, T.; Faruq, H.M.; Laura Magdalena, J.; Manuela, G.; Christopher Horst, L. Role of GSH and Iron-Sulfur Glutaredoxins in Iron Metabolism-Review. *Molecules* **2020**, *25*, 3860. [[CrossRef](#)]
20. Meyer, A.J. The Integration of Glutathione Homeostasis and Redox Signaling. *J. Plant Physiol.* **2008**, *165*, 1390–1403. [[CrossRef](#)]
21. Pai, H.V.; Starke, D.W.; Lesnefsky, E.J.; Hoppel, C.L.; Mieyal, J.J. What Is the Functional Significance of the Unique Location of Glutaredoxin 1 (GRx1) in the Intermembrane Space of Mitochondria? *Antioxid. Redox Signal* **2007**, *9*, 2027–2033. [[CrossRef](#)] [[PubMed](#)]
22. Rouhier, N.; Cerveau, D.; Couturier, J.; Reichheld, J.-P.; Rey, P. Involvement of Thiol-Based Mechanisms in Plant Development. *Biochim. Biophys. Acta* **2015**, *1850*, 1479–1496. [[CrossRef](#)] [[PubMed](#)]
23. Garg, R.; Jhanwar, S.; Tyagi, A.K.; Jain, M. Genome-Wide Survey and Expression Analysis Suggest Diverse Roles of Glutaredoxin Gene Family Members during Development and Response to Various Stimuli in Rice. *DNA Res.* **2010**, *17*, 353–367. [[CrossRef](#)]
24. Xu, H.; Li, Z.; Jiang, P.-F.; Zhao, L.; Qu, C.; Van de Peer, Y.; Liu, Y.-J.; Zeng, Q.-Y. Divergence of Active Site Motifs among Different Classes of Populus Glutaredoxins Results in Substrate Switches. *Plant J.* **2022**, *110*, 129–146. [[CrossRef](#)] [[PubMed](#)]

25. Malik, W.A.; Wang, X.; Wang, X.; Shu, N.; Cui, R.; Chen, X.; Wang, D.; Lu, X.; Yin, Z.; Wang, J.; et al. Genome-Wide Expression Analysis Suggests Glutaredoxin Genes Response to Various Stresses in Cotton. *Int. J. Biol. Macromol.* **2020**, *153*, 470–491. [\[CrossRef\]](#)
26. Boubakri, H.; Najjar, E.; Jihnaoui, N.; Chihaoui, S.-A.; Barhoumi, F.; Jebara, M. Genome-Wide Identification, Characterization and Expression Analysis of Glutaredoxin Gene Family (Grxs) in *Phaseolus Vulgaris*. *Gene* **2022**, *833*, 146591. [\[CrossRef\]](#)
27. Li, T.; Li, M.; Jiang, Y.; Duan, X. Genome-Wide Identification, Characterization and Expression Profile of Glutaredoxin Gene Family in Relation to Fruit Ripening and Response to Abiotic and Biotic Stresses in Banana (*Musa Acuminata*). *Int. J. Biol. Macromol.* **2021**, *170*, 636–651. [\[CrossRef\]](#)
28. Ding, S.; He, F.; Tang, W.; Du, H.; Wang, H. Identification of Maize CC-Type Glutaredoxins That Are Associated with Response to Drought Stress. *Genes* **2019**, *10*, 610. [\[CrossRef\]](#)
29. Gutsche, N.; Thurow, C.; Zachgo, S.; Gatz, C. Plant-Specific CC-Type Glutaredoxins: Functions in Developmental Processes and Stress Responses. *Biol. Chem.* **2015**, *396*, 495–509. [\[CrossRef\]](#)
30. Wang, Z.; Xing, S.; Birkenbihl, R.P.; Zachgo, S. Conserved Functions of Arabidopsis and Rice CC-Type Glutaredoxins in Flower Development and Pathogen Response. *Mol. Plant* **2009**, *2*, 323–335. [\[CrossRef\]](#)
31. Jiang, C.-K.; Ma, J.-Q.; Apostolides, Z.; Chen, L. Metabolomics for a Millenniums-Old Crop: Tea Plant (*Camellia sinensis*). *J. Agric. Food Chem.* **2019**, *67*, 6445–6457. [\[PubMed\]](#)
32. Zhai, X.; Zhang, L.; Granvogl, M.; Ho, C.-T.; Wan, X. Flavor of Tea (*Camellia sinensis*): A Review on Odorants and Analytical Techniques. *Compr. Rev. Food Sci. Food Saf.* **2022**, *21*, 3867–3909. [\[CrossRef\]](#) [\[PubMed\]](#)
33. Liao, Y.; Zhou, X.; Zeng, L. How Does Tea (*Camellia sinensis*) Produce Specialized Metabolites Which Determine Its Unique Quality and Function: A Review. *Crit. Rev. Food Sci. Nutr.* **2022**, *62*, 3751–3767. [\[CrossRef\]](#) [\[PubMed\]](#)
34. Thitimuta, S.; Pithayanukul, P.; Nithitanakool, S.; Bavovada, R.; Leanpolchareanchai, J.; Saparpakorn, P. *Camellia sinensis* L. Extract and Its Potential Beneficial Effects in Antioxidant, Anti-Inflammatory, Anti-Hepatotoxic, and Anti-Tyrosinase Activities. *Molecules* **2017**, *22*, 401. [\[CrossRef\]](#) [\[PubMed\]](#)
35. Xing, L.; Zhang, H.; Qi, R.; Tsao, R.; Mine, Y. Recent Advances in the Understanding of the Health Benefits and Molecular Mechanisms Associated with Green Tea Polyphenols. *J. Agric. Food Chem.* **2019**, *67*, 1029–1043. [\[CrossRef\]](#)
36. Sun, Y.; Zhou, J.; Guo, J. Advances in the Knowledge of Adaptive Mechanisms Mediating Abiotic Stress Responses in *Camellia sinensis*. *Front. Biosci.* **2021**, *26*, 1714–1722. [\[CrossRef\]](#)
37. Xia, E.-H.; Li, F.-D.; Tong, W.; Li, P.-H.; Wu, Q.; Zhao, H.-J.; Ge, R.-H.; Li, R.-P.; Li, Y.-Y.; Zhang, Z.-Z.; et al. Tea Plant Information Archive: A Comprehensive Genomics and Bioinformatics Platform for Tea Plant. *Plant Biotechnol. J.* **2019**, *17*, 1938–1953. [\[CrossRef\]](#)
38. Chen, C.; Chen, H.; Zhang, Y.; Thomas, H.R.; Frank, M.H.; He, Y.; Xia, R. TBtools: An Integrative Toolkit Developed for Interactive Analyses of Big Biological Data. *Mol. Plant* **2020**, *13*, 1194–1202. [\[CrossRef\]](#) [\[PubMed\]](#)
39. Duvaud, S.; Gabella, C.; Lisacek, F.; Stockinger, H.; Ioannidis, V.; Durinx, C. Expasy, the Swiss Bioinformatics Resource Portal, as Designed by Its Users. *Nucleic Acids Res.* **2021**, *49*, W216–W227. [\[CrossRef\]](#) [\[PubMed\]](#)
40. Horton, P.; Park, K.-J.; Obayashi, T.; Fujita, N.; Harada, H.; Adams-Collier, C.J.; Nakai, K. WoLF PSORT: Protein Localization Predictor. *Nucleic Acids Res.* **2007**, *35*, W585–W587. [\[CrossRef\]](#) [\[PubMed\]](#)
41. Kumar, S.; Stecher, G.; Li, M.; Knyaz, C.; Tamura, K. MEGA X: Molecular Evolutionary Genetics Analysis across Computing Platforms. *Mol. Biol. Evol.* **2018**, *35*, 1547–1549. [\[CrossRef\]](#)
42. Letunic, I.; Bork, P. Interactive Tree Of Life (ITOL) v5: An Online Tool for Phylogenetic Tree Display and Annotation. *Nucleic Acids Res.* **2021**, *49*, W293–W296. [\[CrossRef\]](#) [\[PubMed\]](#)
43. Procter, J.B.; Carstairs, G.M.; Soares, B.; Mourão, K.; Ofoegbu, T.C.; Barton, D.; Lui, L.; Menard, A.; Sherstnev, N.; Roldan-Martinez, D.; et al. Alignment of Biological Sequences with Jalview. *Methods Mol. Biol.* **2021**, *2231*, 203–224. [\[CrossRef\]](#) [\[PubMed\]](#)
44. Sievers, F.; Higgins, D.G. Clustal Omega for Making Accurate Alignments of Many Protein Sequences. *Protein Sci.* **2018**, *27*, 135–145. [\[CrossRef\]](#) [\[PubMed\]](#)
45. Waterhouse, A.; Bertoni, M.; Bienert, S.; Studer, G.; Tauriello, G.; Gumienny, R.; Heer, F.T.; de Beer, T.A.P.; Rempfer, C.; Bordoli, L.; et al. SWISS-MODEL: Homology Modelling of Protein Structures and Complexes. *Nucleic Acids Res.* **2018**, *46*, W296–W303. [\[CrossRef\]](#)
46. Shannon, P.; Markiel, A.; Ozier, O.; Baliga, N.S.; Wang, J.T.; Ramage, D.; Amin, N.; Schwikowski, B.; Ideker, T. Cytoscape: A Software Environment for Integrated Models of Biomolecular Interaction Networks. *Genome Res.* **2003**, *13*, 2498–2504. [\[CrossRef\]](#)
47. Wang, Y.; Tang, H.; Debarry, J.D.; Tan, X.; Li, J.; Wang, X.; Lee, T.; Jin, H.; Marler, B.; Guo, H.; et al. MCScanX: A Toolkit for Detection and Evolutionary Analysis of Gene Synteny and Collinearity. *Nucleic Acids Res.* **2012**, *40*, e49. [\[CrossRef\]](#)
48. Lescot, M.; Déhais, P.; Thijs, G.; Marchal, K.; Moreau, Y.; Van de Peer, Y.; Rouzé, P.; Rombauts, S. PlantCARE, a Database of Plant Cis-Acting Regulatory Elements and a Portal to Tools for in Silico Analysis of Promoter Sequences. *Nucleic Acids Res.* **2002**, *30*, 325–327. [\[CrossRef\]](#)
49. Cantalapiedra, C.P.; Hernández-Plaza, A.; Letunic, I.; Bork, P.; Huerta-Cepas, J. EggNOG-Mapper v2: Functional Annotation, Orthology Assignments, and Domain Prediction at the Metagenomic Scale. *Mol. Biol. Evol.* **2021**, *38*, 5825–5829. [\[CrossRef\]](#)
50. Lemaire, S.D. The Glutaredoxin Family in Oxygenic Photosynthetic Organisms. *Photosynth. Res.* **2004**, *79*, 305–318. [\[CrossRef\]](#)

51. Cheng, N.-H.; Liu, J.-Z.; Brock, A.; Nelson, R.S.; Hirschi, K.D. AtGRXcp, an Arabidopsis Chloroplastic Glutaredoxin, Is Critical for Protection against Protein Oxidative Damage. *J. Biol. Chem.* **2006**, *281*, 26280–26288. [[CrossRef](#)]
52. Molina, M.M.; Belli, G.; de la Torre, M.A.; Rodríguez-Manzanique, M.T.; Herrero, E. Nuclear Monothiol Glutaredoxins of *Saccharomyces Cerevisiae* Can Function as Mitochondrial Glutaredoxins. *J. Biol. Chem.* **2004**, *279*, 51923–51930. [[CrossRef](#)]
53. Li, S.; Gutsche, N.; Zachgo, S. The ROXY1 C-Terminal L*LL Motif Is Essential for the Interaction with TGA Transcription Factors. *Plant Physiol.* **2011**, *157*, 2056–2068. [[CrossRef](#)]
54. Zander, M.; Chen, S.; Imkamp, J.; Thürow, C.; Gatz, C. Repression of the Arabidopsis Thaliana Jasmonic Acid/Ethylene-Induced Defense Pathway by TGA-Interacting Glutaredoxins Depends on Their C-Terminal ALWL Motif. *Mol. Plant* **2012**, *5*, 831–840. [[CrossRef](#)] [[PubMed](#)]
55. Lillig, C.H.; Berndt, C.; Holmgren, A. Glutaredoxin Systems. *Biochim. Biophys. Acta* **2008**, *1780*, 1304–1317. [[CrossRef](#)]
56. Navrot, N.; Gelhaye, E.; Jacquot, J.-P.; Rouhier, N. Identification of a New Family of Plant Proteins Loosely Related to Glutaredoxins with Four CxxC Motives. *Photosynth. Res.* **2006**, *89*, 71–79. [[CrossRef](#)] [[PubMed](#)]
57. Jain, M.; Khurana, P.; Tyagi, A.K.; Khurana, J.P. Genome-Wide Analysis of Intronless Genes in Rice and Arabidopsis. *Funct. Integr. Genom.* **2008**, *8*, 69–78. [[CrossRef](#)]
58. Lecharny, A.; Boudet, N.; Gy, I.; Aubourg, S.; Kreis, M. Introns in, Introns out in Plant Gene Families: A Genomic Approach of the Dynamics of Gene Structure. *J. Struct. Funct. Genom.* **2003**, *3*, 111–116. [[CrossRef](#)]
59. Iwamoto, M.; Maekawa, M.; Saito, A.; Higo, H.; Higo, K. Evolutionary Relationship of Plant Catalase Genes Inferred from Exon-Intron Structures: Isozyme Divergence after the Separation of Monocots and Dicots. *Theor. Appl. Genet.* **1998**, *97*, 9–19. [[CrossRef](#)]
60. Louhichi, A.; Fourati, A.; Rebaï, A. IGD: A Resource for Intronless Genes in the Human Genome. *Gene* **2011**, *488*, 35–40. [[CrossRef](#)] [[PubMed](#)]
61. Conant, G.C.; Wolfe, K.H. Turning a Hobby into a Job: How Duplicated Genes Find New Functions. *Nat. Rev. Genet.* **2008**, *9*, 938–950. [[CrossRef](#)] [[PubMed](#)]
62. Xu, G.; Guo, C.; Shan, H.; Kong, H. Divergence of Duplicate Genes in Exon-Intron Structure. *Proc. Natl. Acad. Sci. USA* **2012**, *109*, 1187–1192. [[CrossRef](#)] [[PubMed](#)]
63. Prince, V.E.; Pickett, F.B. Splitting Pairs: The Diverging Fates of Duplicated Genes. *Nat. Rev. Genet.* **2002**, *3*, 827–837. [[CrossRef](#)]
64. Higo, K.; Ugawa, Y.; Iwamoto, M.; Higo, H. PLACE: A Database of Plant Cis-Acting Regulatory DNA Elements. *Nucleic Acids Res.* **1998**, *26*, 358–359. [[CrossRef](#)]
65. Tran, L.-S.P.; Nakashima, K.; Sakuma, Y.; Osakabe, Y.; Qin, F.; Simpson, S.D.; Maruyama, K.; Fujita, Y.; Shinozaki, K.; Yamaguchi-Shinozaki, K. Co-Expression of the Stress-Inducible Zinc Finger Homeodomain ZFHD1 and NAC Transcription Factors Enhances Expression of the ERD1 Gene in Arabidopsis. *Plant J.* **2007**, *49*, 46–63. [[CrossRef](#)] [[PubMed](#)]
66. Higo, K.; Ugawa, Y.; Iwamoto, M.; Korenaga, T. Plant Cis-Acting Regulatory DNA Elements (PLACE) Database: 1999. *Nucleic Acids Res.* **1999**, *27*, 297–300. [[CrossRef](#)]
67. Zhang, X.; Wang, W.; Li, C.; Zhao, Y.; Yuan, H.; Tan, X.; Wu, L.; Wang, Z.; Wang, H. Structural Insights into the Binding of Buckwheat Glutaredoxin with GSH and Regulation of Its Catalytic Activity. *J. Inorg. Biochem.* **2017**, *173*, 21–27. [[CrossRef](#)]
68. Abdalla, M.; Dai, Y.N.; Chi, C.B.; Cheng, W.; Cao, D.D.; Zhou, K.; Ali, W.; Chen, Y.; Zhou, C.Z. Crystal Structure of Yeast Monothiol Glutaredoxin Grx6 in Complex with a Glutathione-Coordinated [2Fe-2S] Cluster. *Acta Crystallogr. F Struct. Biol. Commun.* **2016**, *72*, 732–737. [[CrossRef](#)] [[PubMed](#)]
69. Zhou, J.; Xiong, W.; Wang, Y.; Guan, J. Protein Function Prediction Based on PPI Networks: Network Reconstruction vs Edge Enrichment. *Front. Genet.* **2021**, *12*, 758131. [[CrossRef](#)]
70. Ruan, M.-B.; Yang, Y.-L.; Li, K.-M.; Guo, X.; Wang, B.; Yu, X.-L.; Peng, M. Identification and Characterization of Drought-Responsive CC-Type Glutaredoxins from Cassava Cultivars Reveals Their Involvement in ABA Signalling. *BMC Plant Biol.* **2018**, *18*, 329. [[CrossRef](#)]
71. Ziemann, M.; Bhawe, M.; Zachgo, S. Origin and Diversification of Land Plant CC-Type Glutaredoxins. *Genome Biol. Evol.* **2009**, *1*, 265–277. [[CrossRef](#)] [[PubMed](#)]
72. Kong, H.; Landherr, L.L.; Frohlich, M.W.; Leebens-Mack, J.; Ma, H.; dePamphilis, C.W. Patterns of Gene Duplication in the Plant SKP1 Gene Family in Angiosperms: Evidence for Multiple Mechanisms of Rapid Gene Birth. *Plant J.* **2007**, *50*, 873–885. [[CrossRef](#)] [[PubMed](#)]
73. Li, S.; Lauri, A.; Ziemann, M.; Busch, A.; Bhawe, M.; Zachgo, S. Nuclear Activity of ROXY1, a Glutaredoxin Interacting with TGA Factors, Is Required for Petal Development in Arabidopsis Thaliana. *Plant Cell* **2009**, *21*, 429–441. [[CrossRef](#)] [[PubMed](#)]
74. Xing, S.; Rosso, M.G.; Zachgo, S. ROXY1, a Member of the Plant Glutaredoxin Family, Is Required for Petal Development in Arabidopsis Thaliana. *Development* **2005**, *132*, 1555–1565. [[CrossRef](#)]
75. Michelet, L.; Zaffagnini, M.; Morisse, S.; Sparla, F.; Pérez-Pérez, M.E.; Francia, F.; Danon, A.; Marchand, C.H.; Fermani, S.; Trost, P.; et al. Redox Regulation of the Calvin-Benson Cycle: Something Old, Something New. *Front. Plant Sci.* **2013**, *4*, 470. [[CrossRef](#)]
76. Foyer, C.H.; Noctor, G. Ascorbate and Glutathione: The Heart of the Redox Hub. *Plant Physiol.* **2011**, *155*, 2–18. [[CrossRef](#)]
77. Kumar, A.; Dubey, A.K.; Kumar, V.; Ansari, M.A.; Narayan, S.; Kumar, S.; Pandey, V.; Shirke, P.A.; Pande, V.; Sanyal, I. Overexpression of Rice Glutaredoxin Genes LOC_Os02g40500 and LOC_Os01g27140 Regulate Plant Responses to Drought Stress. *Ecotoxicol. Environ. Saf.* **2020**, *200*, 110721. [[CrossRef](#)] [[PubMed](#)]

78. Wu, Q.; Hu, Y.; Sprague, S.A.; Kakeshpour, T.; Park, J.; Nakata, P.A.; Cheng, N.; Hirschi, K.D.; White, F.F.; Park, S. Expression of a Monothiol Glutaredoxin, AtGRXS17, in Tomato (*Solanum Lycopersicum*) Enhances Drought Tolerance. *Biochem. Biophys. Res. Commun.* **2017**, *491*, 1034–1039. [[CrossRef](#)]
79. Kumar, A.; Kumar, V.; Dubey, A.K.; Ansari, M.A.; Narayan, S.; Meenakshi; Kumar, S.; Pandey, V.; Pande, V.; Sanyal, I. Chickpea Glutaredoxin (CaGrx) Gene Mitigates Drought and Salinity Stress by Modulating the Physiological Performance and Antioxidant Defense Mechanisms. *Physiol. Mol. Biol. Plants* **2021**, *27*, 923–944. [[CrossRef](#)]

Disclaimer/Publisher’s Note: The statements, opinions and data contained in all publications are solely those of the individual author(s) and contributor(s) and not of MDPI and/or the editor(s). MDPI and/or the editor(s) disclaim responsibility for any injury to people or property resulting from any ideas, methods, instructions or products referred to in the content.